UNIVERSIDADE ESTADUAL PAULISTA – UNESP

Faculdade de Ciências Farmacêuticas - Campus de Araraquara

CECÍLIA ALINE OTAVIANO

Subproduto de *Eucalyptus*: obtenção de xilo-oligossacarídeos e avaliação do potencial prebiótico

Araraquara – SP

2026

CECÍLIA ALINE OTAVIANO

Subproduto de *Eucalyptus*: obtenção de xilo-oligossacarídeos e avaliação do potencial prebiótico

Tese apresentada à Universidade Estadual Paulista (UNESP), Faculdade de Ciências Farmacêuticas, de Araraquara, para obtenção do título de Doutora em Alimentos, Nutrição e Engenharia de Alimentos.

Área de Concentração: Alimentos e Nutrição

Orientador: Prof. Dr. Fernando Masarin

Coorientadora: Profa. Dra. Katia Sivieri

Araraquara – SP

2026

Otaviano, Cecília Aline.
O87s Subproduto de *Eucalyptus*: obtenção de xilo-oligossacarídeos e avaliação do potencial prebiótico / Cecília Aline Otaviano. – Araraquara, 2026.
92 f. : il.

Tese (Doutorado) – Universidade Estadual Paulista (UNESP), Faculdade de Ciências Farmacêuticas, Araraquara. Programa de Pós-graduação em Alimentos, Nutrição e Engenharia de Alimentos. Área de concentração: Alimentos e Nutrição.

Orientador: Fernando Masarin.
Coorientadora: Katia Sivieri.

1. *Eucalyptus*. 2. Adsorção. 3. Prebióticos. 4. Antioxidantes. 5. Microbiota intestinal. I. Masarin, Fernando, orient. II. Sivieri, Katia, coorient. III. Título.

Diretoria Técnica de Biblioteca e Documentação - Faculdade de Ciências Farmacêuticas
UNESP - Campus de Araraquara
Kazumi Tomoyose - CRB 8/10904

CAPES: 33004153070P3
Esta ficha não pode ser modificada

CERTIFICADO DE APROVAÇÃO

TÍTULO DA TESE: Subproduto de Eucalyptus: obtenção de xilo-oligossacarídeos e avaliação do potencial prebiótico.

AUTORA: CECILIA ALINE OTAVIANO
ORIENTADOR: FERNANDO MASARIN

Aprovada como parte das exigências para obtenção do Título de Doutora em Alimentos, Nutrição e Engenharia de Alimentos, área: Alimentos e Nutrição pela Comissão Examinadora:

Prof. Dr. FERNANDO MASARIN (Participaçao Presencial)
Departamento de Engenharia de Bioprocessos e Biotecnologia / UNESP / Câmpus de Araraquara - FCF

Profa. Dra. TAIS MARIA BAUAB (Participaçao Presencial)
Departamento de Ciências Biológicas / UNESP / Câmpus de Araraquara - FCF

Prof. Dr. JULIÁN PAUL MARTÍNEZ GALAN (Participaçao Virtual)
Escuela de Nutrición y Dietética / Universidad de Antioquia (UdeA)

Prof. Dr. CASSAMO USSEMANE MUSSAGY (Participaçao Virtual)
Escuela de Agronomia da Facultad de Ciencias Agronómicas y de los Alimentos / Pontificia Universidad Católica de Valparaíso (PUCV) - Chile

Araraquara, 12 de dezembro de 2025.

A vocês, meus pais,
que me ensinaram
a ter raízes fortes
e, ao mesmo tempo,
asas corajosas.
Tudo é também de vocês.
Obrigada por serem abrigo
mesmo quando
ninguém via
a tempestade.

AGRADECIMENTOS

Ao meu padrinho Rodrigo (*in memoriam*), presença que o tempo não apagou. Sua ausência ensinou a saudade, mas sua existência permanece viva em tudo o que me ensinou. Você faz parte dessa conquista.

A minha irmã Cinthia, por ser meu socorro sem hora marcada e por me ensinar a alegria de ver a vida com outros olhos.

Aos meus amigos, em especial aqueles que estiveram ao meu lado durante a pós-graduação, dividindo as dores e vitórias.

Aos velhos, aos novos, aos que passaram e aos que ficaram, a todos. Obrigada.

Aos técnicos de laboratório Ana, Adriana e Ivan, pela paciência, generosidade e apoio.

Ao Prof. Dr. Fernando Masarin, pela orientação e pelo conhecimento compartilhado ao longo de todos esses anos.

À Profa. Dra. Katia Sivieri, pela coorientação, pelo acolhimento e por compartilhar sua experiência.

Ao Prof. Dr. Julián Paul Martínez, por ter me acolhido com tanta generosidade durante meu doutorado sanduíche na Colômbia e a todo o seu grupo de pesquisa, pela parceria e por tornarem o ambiente de trabalho um espaço de crescimento e troca, em especial, aos meus amigos David e Carol.

Ao Programa de Pós-Graduação em Alimentos, Nutrição e Engenharia de Alimentos e ao Departamento de Engenharia de Bioprocessos e Biotecnologia, por toda infraestrutura e suporte técnico que possibilitaram o desenvolvimento deste trabalho.

À Faculdade de Ciências Farmacêuticas – Campus de Araraquara, UNESP, pelo espaço, pela formação e pelas oportunidades científicas e pessoais que contribuíram imensamente para minha formação.

O presente trabalho foi realizado com apoio da Coordenação de Aperfeiçoamento de Pessoal de Nível Superior – Brasil (CAPES) – Código de Financiamento 001.

"O saber a gente aprende com os mestres e os livros.
A sabedoria se aprende é com a vida e com os humildes."

Cora Coralina

RESUMO

A valorização de subprodutos lignocelulósicos é uma das estratégias centrais para o avanço da bioeconomia circular e o desenvolvimento de ingredientes funcionais sustentáveis. Neste contexto, esta tese teve como objetivo obter, purificar e avaliar o potencial prebiótico e antioxidante de uma formulação de xilo-oligossacarídeos (XOS) produzidos a partir de subproduto de *Eucalyptus* proveniente da indústria de celulose e papel. O subproduto de *Eucalyptus* foi submetido a um pré-tratamento hidrotérmico, o hidrolisado foi concentrado por evaporação sob vácuo e, posteriormente, por um processo de adsorção utilizando carvão ativado, visando a remoção de compostos como furfural, hidroximetilfurfural (HMF) e compostos aromáticos derivados da lignina. O carvão ativado demonstrou elevada eficiência na remoção desses compostos, promovendo a redução superior a 90%, com mínima perda da fração de XOS. O processo alcançou índices de purificação entre 68,7-75,2%, com desempenho comparável aos métodos convencionais, porém apresentando vantagens em termos de sustentabilidade, simplicidade operacional e menor impacto ambiental. O potencial funcional dos XOS purificados foi avaliado por ensaios *in vitro*, incluindo crescimento de cepas probióticas, fermentação em *batch in vitro* utilizando microbiota intestinal humana e determinação da atividade antioxidante pelos métodos de 2,2-difenil-1-picrilhidrazil (DPPH) e poder antioxidante redutor férrico (FRAP). Os resultados demonstraram que os XOS obtidos foram capazes de estimular microrganismos benéficos, além de apresentarem atividade antioxidante relevante, indicando seu potencial aplicação como ingrediente funcional em alimentos e produtos nutracêuticos. Portanto, os resultados reforçam que a utilização de subprodutos de *Eucalyptus* para produção de XOS representa uma alternativa tecnológica e ambientalmente viável para agregação de valor, contribuindo para o desenvolvimento de ingredientes funcionais inovadores e sustentáveis.

Palavras-chave: *Eucalyptus*; adsorção; potencial prebiótico; antioxidante; microbiota intestinal.

ABSTRACT

The valorization of lignocellulosic byproducts is one of the central strategies for advancing the circular bioeconomy and developing sustainable functional ingredients. In this context, this thesis aimed to obtain, purify, and evaluate the prebiotic and antioxidant potential of xylooligosaccharides (XOS) produced from *Eucalyptus* byproducts from the pulp and paper industry. *Eucalyptus* byproducts underwent hydrothermal pretreatment, the hydrolysate was concentrated by vacuum evaporation and subsequently by an adsorption process using activated carbon (AC), aiming at the removal of compounds such as furfural, hydroxymethylfurfural (HMF), and aromatic compounds derived from lignin. Activated carbon demonstrated high efficiency in removing these compounds, promoting a reduction of over 90%, with minimal loss of the XOS fraction. The process achieved purification rates between 68.7-75.2%, with performance comparable to conventional methods, however offering advantages in terms of sustainability, operational simplicity, and lower environmental impact. The functional potential of the purified XOS was evaluated by in vitro assays, including the growth of probiotic strains, in vitro batch fermentation using human intestinal microbiota, and determination of antioxidant activity by the 2,2-difenil-1-picrilhidrazil (DPPH) and ferric reducing antioxidant power (FRAP) methods. The results demonstrated that the obtained XOS were able to stimulate beneficial microorganisms, furthermore to exhibiting relevant antioxidant activity, indicating their potential application as a functional ingredient in food and nutraceutical products. The findings reinforce that the use of *Eucalyptus* by-products for XOS production represents a technologically and environmentally viable alternative for adding value, contributing to the development of innovative and sustainable functional ingredients.

Keywords: *Eucalyptus*; adsorption; prebiotic potential; antioxidant; gut microbiota.

LIST OF FIGURES

LIST OF TABLES

1. CHAPTER I

2. CHAPTER II

LIST OF ABBREVIATIONS AND ACRONYMS

Abbreviation	Description
ABTS	2,2′-azino-bis(3-ethylbenzothiazoline-6-sulfonic acid)
CFU	colony-forming units
DP	degree of polymerization
DPPH	2,2-diphenyl-1-picrylhydrazyl
FOS	fructo-oligosaccharides
FRAP	ferric reducing antioxidant power
GOS	galacto-oligosaccharides
HH	hemicellulosic hydrolysate
ISAPP	International Scientific Association for Probiotics and Prebiotics
LLE	liquid–liquid extraction
MOS	mannan-oligosaccharides
HP	hydrothermal pretreatment
SCFAs	short-chain fatty acids
XOS	xylo-oligosaccharides
AC	activated charcoal

LIST OF SYMBOLS

Symbol	Description
β-(1→4)	Type of glycosidic linkage between monosaccharides (from carbon 1 of one unit to carbon 4 of the next, with beta configuration)
°C	Degrees celsius (unit of temperature)
%	Percentage
$g \cdot mol^{-1}$	Grams per mole (unit of molar mass)
pH	Hydrogen potential (measure of the acidity or basicity of a solution)
X2, X3, …	Nomenclature for different xos according to the number of xylose units (e.g., X2 = xylobiose, X3 = xylotriose etc.)

SUMMARY

1 INTRODUTION

The growing global concern with quality of life and health promotion has driven the development of functional foods and bioactive ingredients with beneficial effects on the human body. In this context, prebiotics have gained prominence, especially those obtained from renewable and sustainable sources, such as agro-industrial byproducts. Among the compounds with recognized prebiotic potential, xylooligosaccharides (XOS) stand out for their ability to positively modulate the gut microbiota, their physicochemical stability, and the possibility of obtaining them from lignocellulosic materials rich in hemicellulose, such as byproducts of *Eucalyptus* processing (Corim Marim; Gabardo, 2021; Gibson et al., 2017).

Eucalyptus wood is widely cultivated in South American countries, being the main source of fibers to produce pulp and paper. Brazil, the world's third-largest pulp producer and a global leader in exports, reached a production of approximately 25 million tons of pulp and 11 million tons of paper in 2023, consolidating its strategic position in the industrial forestry sector (Relatório Ibá, 2024). The industrial processing of *Eucalyptus* generates a significant amount of byproducts, such as slabs, offshoots, shavings, bark, sawdust, and wood chips, which represent an environmental liability but also an opportunity for valorization through their bioproducts conversion of nutritional and industrial interest (Xavier *et al.*, 2025).

The *Eucalyptus* byproduct (sawdust) used in this thesis is obtained from the *Eucalyptus* logs conversion into wood chips, an initial step in the production of cellulose pulp, one of the main byproducts of this sector. It is composed mainly of lignin, cellulose, and hemicellulose, making it a raw material with great potential to produce high value-added compounds, such as XOS.

The chemical composition of *Eucalyptus* wood can be classified into low and high molar mass fractions. The low molar mass fraction includes organic substances, known as extractives, and inorganic substances, generally represented by salts of metallic ions. Extractives encompass a wide variety of chemical compounds that can be removed by organic solvents, although some are also water-soluble. These compounds, present in small quantities (approximately 2-8%, w/w, dry weight), are responsible for the sensory

characteristics of the wood, such as odor, color, and flavor. Among the main extractives are waxes, flavonoids, terpenes, lignans, and fatty acids. Inorganic compounds, found in even smaller proportions (1-2%, w/w, dry weight), also make up the low molar mass fraction of lignocellulosic materials (Ek; Gellerstedt; Henriksson, 2009; Paz-Cedeno, 2022).

Macromolecules represent almost the entire composition of *Eucalyptus* wood and are essentially composed of three main classes: cellulose, polysaccharides (also denominated hemicelluloses), and lignin. Among these, cellulose (Figure 1) stands out as the major component, corresponding to approximately 40% (w/w, dry weight). It is a linear polysaccharide of high molar mass, formed exclusively by units of anhydro-D-glucose linked by β-(1→4) glycosidic bonds, forming a dimer known as cellobiose, which is the repeating unit of cellulose, organized in crystalline and amorphous regions along the polymer chain (Ek; Gellerstedt; Henriksson, 2009; Paz-cedeno, 2022).

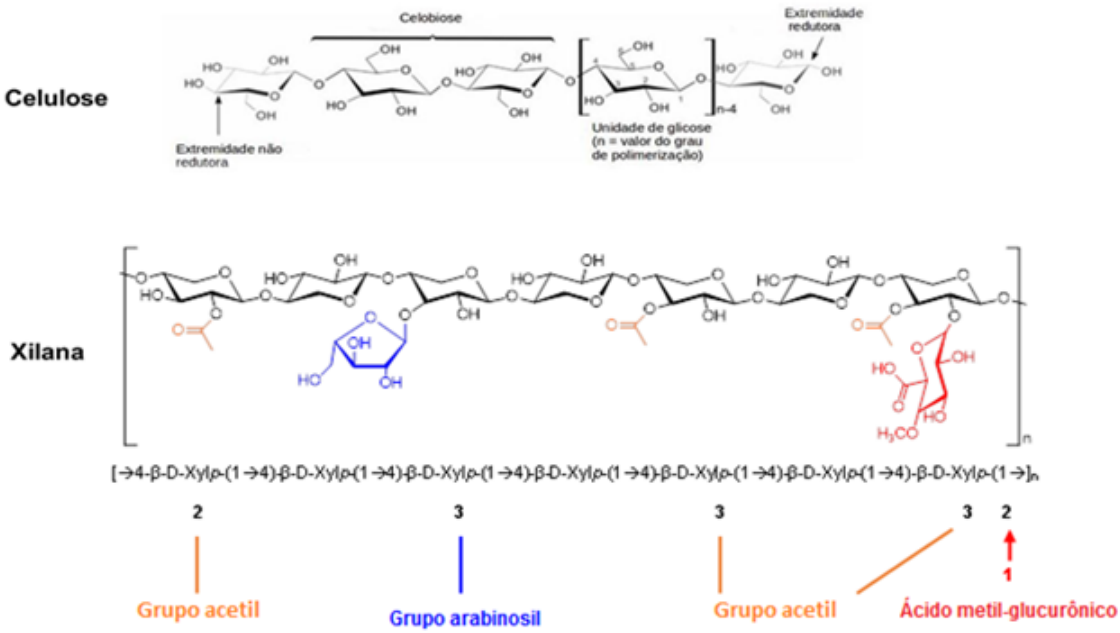

Figure 1. Molecular structure of cellulose and structure of L-arabino-D-xylan, the main hemicellulose constituent in sugarcane by-products (Adapted from Paz-Cedeno, 2022).

The molar mass of cellulose can vary significantly, ranging from 50,000 to 2.5 million $g \cdot mol^{-1}$, depending on the botanical origin and processing of the material. As it is a true polymer, its size is commonly expressed by the degree of

polymerization (DP), defined as the ratio between the average molar mass of the polymer and the molar mass of the repeating anhydroglucose unit. A distinctive characteristic of cellulose is its ability to form extensive intra- and intermolecular hydrogen bond networks, resulting in the formation of highly organized microfibrils. In the context of the cell wall of lignocellulosic biomass, these microfibrils are organized in parallel and embedded in a matrix composed of hemicelluloses and lignin, providing structural rigidity and cohesion to the plant tissue (Ek; Gellerstedt; Heriksson, 2009).

Eucalyptus hemicellulose is mainly composed of the xylan molecule (a homopolysaccharide). Xylan has a main chain consisting of β-(1→4)-D-xylopyranosyl residues, with side groups attached to the β-(1→4)-D-xylopyranosyl residue at certain points along the main chain, such as arabinosyl groups (α-L-arabinoxylan), acetyl groups, and methylglucuronic acid (4-O-methyl) (Bian et al., 2013; Buckeride, 2017; Ek; Gellerstedt; Henriksson, 2009; Paz-Cedeno, 2022; Xiao; Song; Sun, 2017).

Lignin is a macromolecule composed of three main types of hydroxycinnamyl alcohols: p-coumaric alcohol, coniferyl alcohol, and sinapyl alcohol. When polymerized, these monolignols are referred to as lignin monomeric units, as follows: p-hydroxyphenyl (H unit), guaiacyl (G unit), and syringyl (S unit). These monomeric units are irregularly chemically connected by a variety of carbon-carbon and ether bonds, the most common being arylglycerol-β-aryl (β-O- (Buckeridge, 2017). The proportion of lignin constituents varies according to cell type, plant tissues, and plant species. Hardwood lignin (including *Eucalyptus*) is composed mainly of GS units (Figure 2) (10,11). *Eucalyptus* lignin is located primarily in vascular bundles (cell walls of vessel cells and fibers) and in smaller quantities in the cell walls of parenchyma cells, which store starch. (Buckeride, 2017). The xylan molecule is chemically linked to lignin via methylglucuronic acid (side group) and directly to the xylose units of the (Figure 2) (Buckeride, 2017; Paz-Cedeno, 2022).

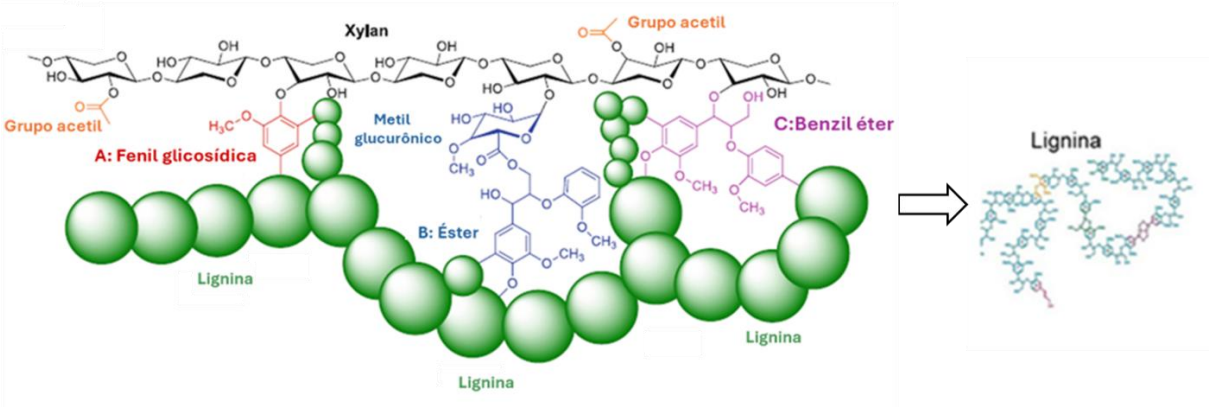

Figure 2. Diagram representing the typical bonds between hardwood hemicellulose and lignin. A: Phenyl glycosidic bond. B: Ester bond. C: Benzyl ether bond. In the case of bond B, methylglucuronic acid bridges the hemicellulose and lignin (Paz-Cedeno, 2022).

XOS are oligomers composed of xylose units linked by β-(1→4) glycosidic bonds. These compounds are mainly obtained from the hemicellulosic fraction of lignocellulosic materials (hardwoods and grasses), often derived from agro-industrial byproducts such as corn cobs, rice husks, almonds, olive pomace, barley, and oat (Aachary; Prapulla, 2011). They exhibit a degree of polymerization (DP) between 2-12, with the most common forms being xylobiose (X2), xylotriose (X3), xylotetraose (X4), xylopentaose (X5), and xylohexaose (X6) (Figure 3). The structural composition of XOS can vary according to the plant source and hydrolysis conditions, sometimes presenting substituents such as acetyl, arabinosyl, and methyl-glucuronic acid groups, which influence their physicochemical and functional properties (Aaachary; Prapulla, 2011; LI et al., 2022).

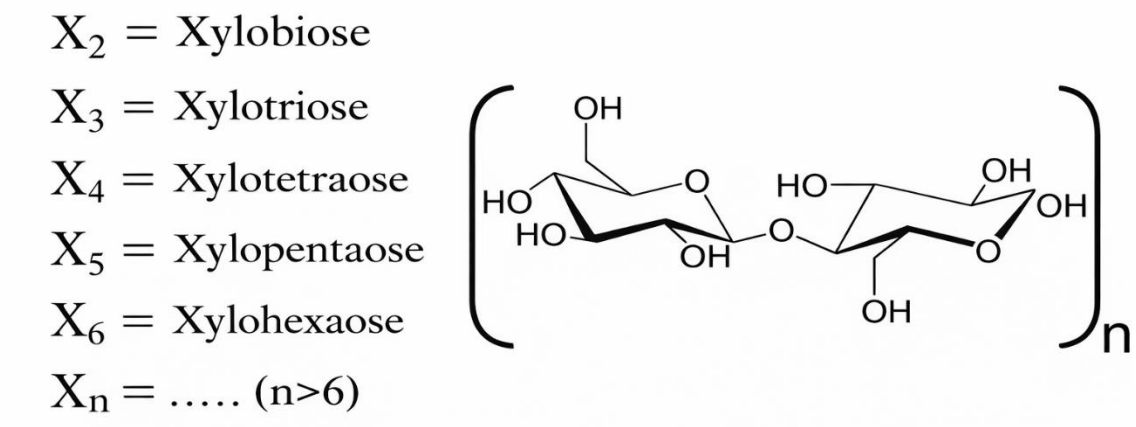

Figure 3. Structure of xylo-oligosaccharides (XOS).

Source: Prepared by the author.

XOS have a wide range of applications, primarily in the food, pharmaceutical, and agricultural sectors. In the food sector, they have been used as functional ingredients in yogurts, biscuits, beverages, supplements, and infant formulas, acting as prebiotics by selectively promoting the growth of beneficial microorganisms in the gut, such as Bifidobacterium and Lactobacillus (Gibson et al., 2017).

Furthermore to their prebiotic effect, XOS offer technological advantages such as low calorie content, absence of cariogenicity, moderate sweetness, broad stability at pH 2.5-8 (allowing their use in products with extended shelf life) and temperature up to 100°C, as well as conferring favorable sensory properties to foods (Gibson et al., 2017; Moure et al., 2006; Samanta et al., 2015).

Although they occur naturally in small amounts in fruits, vegetables, and honey, XOS have demonstrated significant prebiotic effects, such as selectively stimulating the growth of bifidobacteria and other beneficial microorganisms in the gastrointestinal tract.

The definition of prebiotics has been updated by the International Scientific Association for Probiotics and Prebiotics (ISAPP) and is now defined as: “substrates that are selectively utilized by host microorganisms to confer health benefits” (Deehan et al., 2024; Gibson et al., 2017). Therefore, XOS are part of a group of functional compounds capable of positively modulating the gut microbiota, which makes them especially attractive for application in foods aimed at gut health, immunity, and the prevention of metabolic diseases.

Although prebiotics are classically carbohydrates, such as inulin, fructooligosaccharides (FOS), galactooligosaccharides (GOS), mannanoligosaccharides (MOS), and XOS, containing 2-12 monosaccharide units of the main chain linked by α- or β-glycosidic bonds, in linear or side-groups form, other non-carbohydrate compounds have also been reported in the literature as prebiotics, including polyphenols, minerals, and polyunsaturated fatty acids (Leone; Ferrante, 2023; Neri-numa; Pastore, 2020).

In Japan, XOS are already widely used in commercial products such as infant food, formula for the elderly, yogurt, pasta, and beverages, representing a consolidated market with a demand of approximately 650 tons per year (Vázquez., 2001). Furthermore to their use in food, these compounds have been investigated for their antioxidant and anti-allergic properties, and for their potential in pharmaceutical and agriculture (Crittenden, Playne., 1996).

Prebiotics are considered non-digestible substrates that serve as a fermentation source for intestinal microorganisms, leading to the production of short-chain fatty acids (SCFAs) such as acetate, propionate, and butyrate. These metabolites reduce intestinal pH and promote the growth of beneficial bacteria, such as Bifidobacterium spp. and Lactobacillus spp. In diets, digestible carbohydrates are absorbed in the small intestine, while non-digestible carbohydrates are metabolized by bacteria in the colon, resulting in the production of SCFAs (Leone; Ferrante, 2023).

The main prebiotics are generally insoluble fibers extracted from plants, legumes, grains, vegetables, and cruciferous fruits. Although they do not have direct nutritional value, they perform important physiological functions, such as stimulating intestinal motility and modulating the composition of the intestinal microbiota, which justifies their inclusion in diets (Leone; Ferrante, 2023).

Finally, for a substrate to be classified as a prebiotic, its beneficial health effects must be scientifically proven through well-controlled clinical trials. The current definition aims to promote the appropriate and consistent use of the term "prebiotic" among the various stakeholders involved, such as consumers, suppliers, researchers, regulatory bodies, and the media, ensuring clarity in scientific and commercial communications (Gibson et al., 2017).

The main objective of using prebiotics is to promote health and reduce the risk of disease. The most effective approaches are those based on prevention, through strategies that favor the development of a diverse and balanced microbiota. For a prebiotic to meet the criterion of providing health benefits, controlled trials are necessary to establish a direct relationship between the compound and positive effects on the target host. Furthermore, the level of evidence required must be proportional to the robustness of the benefit claim (Deehan et al., 2024; Gibson et al., 2017).

Several randomized clinical trials have already demonstrated the beneficial effects of different prebiotics, both in healthy individuals and in patients with acute or chronic diseases. However, it is important to highlight that the effects of any intervention can be modulated by environmental variables and individual host characteristics, which contributes to the variability in clinical responses observed among study participants (Gibson et al., 2017).

The effective use of prebiotics depends on the presence, in the host microbiota, of microorganisms capable of metabolizing them. This dependence may explain the interindividual heterogeneity in responses to prebiotic treatments. Intrinsic host factors, such as genetic predisposition, polymorphisms in microbial recognition pathways, and susceptibility to certain diseases, can influence the composition of the microbiota and the biological effects of supplementation. In parallel, environmental factors, such as type of delivery, nutrition in the first years of life, antibiotic use, health conditions, and dietary habits, also play a significant role in modulating the human microbiome and, consequently, in the effects of prebiotic ingestion (Gibson et al., 2017).

More recent studies have further expanded the potential uses of XOS, including applications in the production of biodegradable materials such as water-soluble films, capsules, hydrogels, and renewable-source plastics. Furthermore, bioactive properties such as anti-inflammatory, antioxidant, and anticancer activity have been investigated, opening new possibilities in the pharmaceutical and biomedical fields (Alvarez; Fernandéz; Ciancia, 2024; Manicardi et al., 2023; Nogueira-Prieto et al., 2025).

The valorization of lignocellulosic byproducts, such as *Eucalyptus* byproducts to produce XOS, represents a sustainable and economically

attractive alternative. Commercially pure XOS are sold for between US$ 20-50 per kilogram of product, values that exceed those of cellulose pulp or energy generated from these byproducts, highlighting the high added value of XOS (Valladares-Diestra *et al.*, 2023a). However, obtaining XOS requires hydrolysis technologies for the xylan molecule (chemical or enzymatic), and achieving high yield and purity (≥ 95%) necessitates a downstream purification process of the obtained hemicellulosic hydrolysate (HH), which presents considerable technical and economic challenges.

Given their promising structural and functional characteristics, XOS have been extensively studied regarding their production, purification, and application methods. In this context, different methods have been employed to enable the production of XOS from lignocellulosic biomass, including *Eucalyptus* byproducts. XOS production can be carried out by chemical, enzymatic, autohydrolytic methods, as well as combined approaches. Hydrothermal pretreatment (HP), based on the autohydrolysis of hemicellulose, stands out as one of the most promising strategies, allowing the controlled release of the hemicellulosic fraction under controlled temperature (120-190°C) and time (30-110 min) conditions. HP culminates in an XOS-rich HH depending on the temperature and time conditions; however, other compounds derived from lignocellulosic biomass, such as monomeric sugars, organic acids, and lignin derivatives, are also generated in the HH. The efficiency of the process can be measured using the process severity factor (P-factor), which considers operational parameters and is directly linked to the conversion of xylan into XOS (Chen *et al.*, 2018; Mhetras; Mapre; Gokhale, 2019; Neto *et al.*, 2020; Qin *et al.*, 2022).

For XOS-rich hydrolysates to be suitable for application in the food and nutraceutical industries, it is necessary to remove the impurities generated during HP. The purification of XOS-rich hydrolysates involves several steps, including evaporation, precipitation, liquid-liquid extraction (LLE), chromatography, and drying (Otaviano et al., 2023; Moure et al., 2006). The literature, however, still lacks studies that systematically evaluate different purification strategies applied specifically to lignocellulosic biomass, especially focusing on obtaining high-purity XOS for application as a prebiotic (Cebreiros; Guigou; Cabrera, 2017).

For the purification of the obtained XOS, activated carbon has emerged as a promising alternative due to its high surface area, high adsorption capacity, and selectivity for undesirable compounds such as phenols, organic acids, and dyes, while preserving the structure of the oligosaccharides (Ahmed; Liml, 2021; Dabrowski *et al.*, 2005). The use of activated carbon (AC) is considered an economical, sustainable, and relatively simple method compared to other techniques, such as chromatography, making it suitable for industrial-scale application (Kruschitz; Nidetzky, 2020). In this work, activated carbon was investigated as a novel approach for the purification of XOS obtained from *Eucalyptus* byproducts by HP.

To validate their beneficial health effects, several in vitro models have been used as a preliminary step to clinical analyses, allowing for the controlled simulation of the intestinal environment and the observation of microbial, physiological, or chemical responses associated with the use of these compounds (Sivieri *et al.*, 2014).

Among the strategies used to evaluate the prebiotic potential of XOS, the assessment of the growth of pure probiotic strains in media containing XOS as a carbon source stands out. This type of assay allows observing, under controlled conditions, the ability of different beneficial microorganisms to metabolize XOS, comparing growth curves obtained by turbidity or optical density measurements (OD 600), colony-forming unit (CFU) counts, or molecular techniques (De Freitas; Carmona; Brienzo, 2019; Lasrado; Gudipati, 2015). This approach was evaluated for purified XOS obtained from *Eucalyptus* byproduct by PTH.

Another widely used approach to evaluate the prebiotic potential of XOS involves batch fermentation, which consists of a closed system in which an inoculum of human gut microbiota, usually obtained from the feces of healthy donors, is cultivated in a specific medium containing XOS as a carbon source, under strictly anaerobic conditions and a temperature of 37 °C. This model allows monitoring changes in microbial composition, SCFA production, and parameters such as pH over 24-48 h. It is a robust, reproducible, and low-cost tool, widely used in screening assays to assess the prebiotic potential prior to conducting in vivo studies (Sivieri *et al.*, 2014). Despite its simplicity, batch fermentation provides valuable data on fermentability and its initial impact on specific bacterial

populations, such as Bifidobacterium and Lactobacillus. This approach was investigated in this work to evaluate the prebiotic effect of purified XOS obtained from Eucalyptus byproduct by HP.

Alongside microbial evaluations, the bioactive properties of XOS have also been explored, such as antioxidant activity, which can contribute to protection against oxidative stress at the intestinal and systemic levels. For this purpose, assays such as DPPH (2,2-diphenyl-1-picrylhydrazyl) and FRAP (ferric reducing power) are commonly used to measure the ability of XOS to trap free radicals or donate electrons (Alvarez; Fernandez; Ciancia, 2024). There is evidence that the antioxidant activity of XOS can be enhanced when combined with probiotic strains, creating symbiotic preparations with expanded functional action (YU *et al.*, 2015). This approach was also investigated in this work with purified XOS obtained from *Eucalyptus* byproduct by HP.

The evaluation of the prebiotic effect of XOS, in turn, will be carried out using the product previously refined through evaporation and liquid-liquid extraction (LLE) techniques, as developed in a previous study by the research group (Otaviano et al., 2023). This in vitro evaluation, involving the selective cultivation of beneficial microorganisms such as bifidobacteria and lactobacilli, allowed for the monitoring of parameters such as bacterial growth, SCFA production, and modulation of the simulated microbiota (Ávarez *et al.*, 2023; Yao *et al.*, 2022).

Furthermore, this thesis was structured in the format of chapters corresponding to scientific articles, aiming to organize and highlight the different stages of the work developed. Initially, the HH obtained from the HP of *Eucalyptus* by-products was subjected to refining processes by evaporation and LLE, resulting in a fraction enriched in XOS (XOS-extract). This purified material, described by Otaviano et al., 2023 "*Hydrothermal pretreatment of Eucalyptus by-product and refining of xylooligosaccharides from hemicellulosic hydrolysate"* https://doi.org/10.1016/j.seppur.2022.122520). It was used in in vitro assays to evaluate the prebiotic and antioxidant effect, generating results that culminated in the preparation of the subsequent article [Chapter II "*Xylooligosaccharides obtained from the hydrothermal pretreatment of Eucalyptus by-product as functional ingredients with dual function: prebiotic and antioxidant potential*".

Subsequently, aiming to optimize the recovery and purity of the XOS, a purification method based on AC was developed, demonstrating high efficiency in refining the HH. The application of this method resulted in a product with greater functional potential, the evaluation of which was reported in a subsequent scientific article [Chapter I "*Purification of xylooligosaccharides from Eucalyptus by-product using activated carbon adsorption*" (Submitted to the journal Bioresource Technology Reports). Therefore, this thesis integrates both the prebiotic and antioxidant effect of the previously purified extract (XOS-extract) and the development and validation of an innovative methodological approach for obtaining purified XOS, contributing to the valorization of by-products from the pulp and paper industry and to the advancement of knowledge about functional ingredients of interest in the food sector.

2 OBJECTIVE

This thesis main aimed to assess refining strategies and the prebiotic potential of a XOS-extract obtained from a *Eucalyptus* byproduct. Therefore, the specific objectives established to achieve the goal of this thesis are as follows:

- Obtain an XOS-extract from HP of *Eucalyptus* byproduct;
- Refine and dry the previously obtained XOS-extract using evaporation and LLE techniques;
- Assess the prebiotic effect and antioxidant activity of the previously obtained XOS-extract through in vitro assays;
- Investigate the prebiotic effect of the previously obtained XOS-extract through in vitro batch;
- Assess fermentation with human gut microbiota from healthy adults of the previously obtained XOS-extract;
- Assess the refining of XOS obtained by HP of *Eucalyptus* byproduct using adsorption and desorption techniques on AC;

CHAPTER I

Purification of xylooligosaccharides from *Eucalyptus* by-product using activated carbon adsorption

Cecília Aline Otaviano,[1] Cassamo Ussemane Mussagy,[2] Fernando Masarin,[1*]

[1]São Paulo State University (UNESP), School of Pharmaceutical Science (FCF), Department of Bioprocess Engineering and Biotechnology. Araraquara-SP, Brazil. 14800-903

[2]Laboratorio de Desarrollo de Bioprocesos Sostenibles (Labisost), Escuela de Agronomía, Facultad de Ciencias Agronómicas y de los Alimentos, Pontificia Universidad Católica de Valparaíso, Casilla 4-D, Quillota 2260000, Chile.

(*) Corresponding author

Email addresses:

CAO: cecilia.otaviano@unesp.br
CUM: cassamo.mussagy@pucv.cl
FM: fernando.masarin@unesp.br

ABSTRACT

The valorization of lignocellulosic by-products represents a sustainable route to obtain bioactive compounds of industrial interest. In this study, the production and purification of xylooligosaccharides (XOS) from *Eucalyptus* byproduct were investigated through hydrothermal pretreatment followed by adsorption on activated carbon (AC). The hemicellulosic hydrolysate (HH) was concentrated and subjected to varying activated carbon dosages (0.005, 0.025, 0.050, and 0.100 g), followed by desorption using aqueous ethanol solutions (15, 30, and 50%) and water. The fractions were analyzed by high-performance liquid chromatography (HPLC) and UV-Vis spectrophotometry for quantification of XOS, monosaccharides, furans, and total aromatics. AC characterization revealed a high surface area, acidic surface functional groups, and a porous morphology suitable for purification processes. AC efficiently removed inhibitory compounds such as hydroxymethylfurfural (HMF), furfural, and total aromatics, while preserving a significant fraction of XOS. Desorption with 30% ethanol selectively recovered oligomers while reducing monosaccharides and colored impurities. These results demonstrate the potential of AC as a low-cost and environmentally friendly adsorbent for XOS purification. The proposed strategy can be integrated into biorefineries to add value to cellulose and paper industry wastes, fostering the production of functional ingredients for food, nutraceutical, and pharmaceutical applications.

Keywords: Activated carbon; Xylooligosaccharides; Purification; *Eucalyptus* byproduct; Adsorption; Ethanol desorption.

HIGHLIGHTS

- Hemicellulose hydrolysate was refined using activated carbon adsorption.
- Efficient adsorption of inhibitory compounds (hydroxymethylfurfural, furfural, and total aromatics).
- Selective recovery of XOS with 30% ethanol desorption.
- Sustainable strategy for the valorization of cellulose industry wastes.

1. INTRODUCTION

The transition toward a circular bioeconomy demands innovative strategies to convert industrial byproducts into high added value bioproducts. Among renewable feedstocks, lignocellulosic biomass stands out as an abundant and low-cost source of carbohydrates that can be upgraded into functional ingredients, fuels, and biochemicals. *Eucalyptus* byproduct generated by the pulp and paper industry, such as sawdust, represent a largely untapped resource rich in hemicellulose. Leveraging these by-products aligns with global sustainability goals while opening new technological routes for producing bioactive compounds of industrial relevance (Carvalho *et al.*, 2013; Moure *et al.*, 2006). Xylooligosaccharides (XOS) are short xylose polymers derived from hemicellulose hydrolysis, typically containing 2-12 xylose units. Over the past decade, its XOS has attracted increasing attention as next-generation prebiotics with demonstrated benefits for gut health, immune modulation, and oxidative balance. They selectively stimulate beneficial bacteria such as *Bifidobacterium* and *Lactobacillus*, enhance short-chain fatty acid (SCFA) production, and exhibit anti-inflammatory and cholesterol-lowering effects (Aantov; Đordevic, 2017; Xu *et al.*, 2019; Zhang, Xiankun *et al.*, 2020). These properties make XOS promising ingredients for functional foods, nutraceuticals, and pharmaceutical formulations. However, their biological efficacy depends critically on purity: the presence of monosaccharides, aromatics compounds, furans, and colored impurities can compromise both functionality and safety (Xu *et al.*, 2019).

Commercial extraction of XOS from natural sources such as honey or fruits is economically unfeasible due to their low abundance. In contrast, hemicellulose-rich lignocellulosic by-product from *Eucalyptus* offer an attractive alternative feedstock (Manicardi *et al.*, 2023; Vázquez *et al.*, 2000). Brazil, the world's largest pulp exporter, produces millions of tons of *Eucalyptus* by-product annually, most of which remain underutilized. According to the Brazilian Tree Industry (IBÁ), over 1.8 million trees are planted daily for pulp production (Relatório Ibá 2024). Converting this material into high-purity XOS therefore integrates environmental responsibility with economic opportunity, reinforcing the biorefinery concept. Despite this potential, the purification of XOS from hemicellulosic hydrolysates (HH) remains a major bottleneck. Hydrothermal or

enzymatic treatments generate complex mixtures containing not only oligomers but also furfural, hydroxymethylfurfural (HMF), weak acids, and aromatics compounds known to inhibit microbial growth and downstream bioconversion (CARVALHO *et al.*, 2013; MOURE *et al.*, 2006). Developing efficient, low-cost, and environmentally friendly purification strategies is thus essential for the industrial viability of XOS production (Future Market Insights, 2023; Samanta *et al.*, 2015).

Activated carbon (AC) adsorption has emerged as one of the most promising technologies for hydrolysate detoxification and oligosaccharide refinement. Owing to its large surface area, adjustable pore size distribution, and tunable surface chemistry, AC offers selective adsorption toward aromatic and hydrophobic inhibitors while preserving carbohydrates (Tamayo-Pena *et al.*, 2024; Xu *et al.*, 2019). Furthermore, it is inexpensive, regenerable, and compatible with green processing routes, enabling integration into sustainable biorefineries. Previous studies have demonstrated the effectiveness of AC in removing furans and aromatics compounds from lignocellulosic hydrolysates (Nobre; Teixeira; Rodrigues, 2012; Zhu *et al.*, 2021). However, the adsorption-desorption behavior of XOS on AC surfaces remains poorly understood, particularly regarding selectivity among oligomers of different degrees of polymerization and the influence of solvent polarity (Otaviano *et al.*, 2023; Paschoa *et al.*, 2024; Zhang *et al.*, 2018).

Addressing these gaps, the present study investigates the use of AC for the purification of XOS derived from *Eucalyptus* by-product hydrolysates. A hydrothermal pretreatment was applied to release hemicellulosic fractions, followed by adsorption on AC and desorption using ethanol-water mixtures of varying concentrations. Comprehensive chromatographic and spectroscopic analyses were conducted to assess the removal of inhibitory compounds and the selective recovery of XOS. This work aims to provide mechanistic insights and practical evidence supporting AC as a low-cost, sustainable adsorbent for integrating XOS purification into modern biorefineries.

2. MATERIAL AND METHODS

2.1. Feedstock and hemicellulosic hydrolysate (HH) production

The HH was obtained from *Eucalyptus* by-product generated during log cutting in the pulp and paper industry. The feedstock consisted of a 1:1 (w/w) mixture of *Eucalyptus grandis* and *Eucalyptus urophylla*. Hydrothermal pretreatment was carried out in a Regmed™ stainless-steel reactor equipped with mechanical agitation and temperature and pressure control. Each batch contained 50 g (dry weight) of *Eucalyptus* by-product and 500 mL of distilled water (10% w/v). The reactor was heated to 160 °C over approximately 40 min and maintained at this temperature for 65 min. After natural cooling (~6 h), the resulting HH was filtered through a sintered glass filter (porosity number 3) and stored at −20 °C until use, as described by Otaviano et al. (2023) (Otaviano *et al.*, 2023). This process yielded a HH enriched in XOS, monomeric sugars, and soluble aromatic compounds.

2.2. Concentration of the hemicellulosic hydrolysate (HH) by vacuum evaporation

To remove volatile components and concentrate the oligosaccharides, the HH was subjected to vacuum evaporation following the protocol described by Otaviano et al. (2023) (Otaviano *et al.*, 2023). The process was conducted in a stainless-steel rotary evaporator (Heidolph) at 50 °C under 200 mbar for 10 min, followed by 100 mbar for 50 min. After concentration, the sample volume was measured, transferred to polypropylene bottles, and stored at −20 °C until further analysis.

2.3. Adsorption on activated carbon (AC)

The refinement of XOS using AC was performed according to Zhang et al. (2018) and Paschoa et al. (2024), with minor modifications (Paschoa *et al.*, 2024; Zhang *et al.*, 2018). AC dosages of 0.005, 0.025, 0.050, and 0.100 g were added to 5 mL of concentrated HH in 15 mL Falcon tubes. The mixtures were agitated at 150 rpm and 30 °C for 1 h using a benchtop shaker. After centrifugation, the supernatant was carefully separated, measured, and stored at −20 °C until analysis. These conditions were selected to simulate small-scale adsorption while minimizing sugar degradation and volatilization.

2.4. Desorption with solvent mixtures

Following adsorption, desorption was carried out using ethanol-water mixtures at different concentrations (15, 30, and 50%, v/v) and distilled water as control. 5 mL of solvent were added to each AC-containing tube. The suspensions were agitated and centrifuged under the same conditions as the adsorption step (150 rpm, 30 °C, 1 h) to promote desorption of adsorbed compounds (Zhang *et al.*, 2018). The supernatant fractions containing the desorbed compounds were collected, measured, and stored at −20 °C for subsequent chromatographic and spectrophotometric analyses.

2.5. Analytical Methods

2.5.1. Determination of XOS and xylose

XOS and xylose concentrations were determined by high-performance liquid chromatography (HPLC, Shimadzu NEXERA XR) equipped with a BIO-RAD Aminex HPX-87C column (300 × 7.8 mm). The column temperature was maintained at 80 °C, and ultrapure water was used as the mobile phase at 0.6 mL min^{-1}. Injection volume was 20 µL, and a refractive index detector (Shimadzu RID-20A) was operated at 60 °C. Samples were adjusted to pH 6.5 with 1 M NaOH, filtered through SEP-PACK C18 cartridges and 0.45 µm membranes prior to injection. Analytical standards included xylose (X1), xylobiose (X2), xylotriose (X3), xylotetraose (X4), and higher oligomers (XOS>6) prepared from Megazyme (Ireland) standards. Analytical curves were constructed using analytical-grade standards (Sigma-Aldrich (X1) and Megazyme-Ireland (X2- XOS>6) dried under phosphorus pentoxide and vacuum. All analyses were performed in triplicate (Otaviano *et al.*, 2023; Mafei *et al.*, 2020).

2.5.2. Determination of furfural and hydroxymethylfurfural (HMF)

Furfural and HMF were quantified by HPLC (Shimadzu NEXERA XR) using a Hypersil ODS C18 column (250 × 4 mm, 5 µm, 120 Å; Thermo). The mobile phase consisted of acetonitrile:water (1:8 v/v) containing 1% (w/v) acetic

acid. The flow rate was 0.8 mL min^{-1}, detection wavelength 276 nm, and column temperature 25 °C. Injection volume was 20 µL, and the analysis time was 12 min. Analyses were performed in triplicate. All measurements were conducted in triplicate using analytical-grade standards (Sigma-Aldrich) (Otaviano *et al.*, 2023; Mafei *et al.*, 2020).

2.5.3. Determination of total aromatic compounds

Total soluble aromatics were determined spectrophotometrically at 280 nm using a UV-Visible spectrophotometer (Thermo Scientific Genesys 10S). Concentrations were calculated using a molar extinction coefficient of 20 Lg^{-1} cm^{-1} (Antov-Dordevic, 2017). Analyses were performed in triplicate.

2.5.4. Determination of monosaccharides and organic acids

Monomeric sugars (glucose, arabinose) and organic acids (formic and acetic acids) were quantified by HPLC (Shimadzu NEXERA XR) with a BIO-RAD Aminex HPX-87H column (300 × 7.8 mm). The column temperature was maintained at 60 °C, using 5 mM H_2SO_4 as mobile phase (0.6 $mLmin^{-1}$). The detector was a refractive index unit (RID-20A) operating at 60 °C with an analysis time of 17 min. Samples were filtered through SEP-PACK C18 cartridges and 0.45 µm membranes prior to injection. Analyses were performed in triplicate. Analytical standards were of reagent grade (Sigma-Aldrich), dried under vacuum and P_2O_5 before use (Otaviano *et al.*, 2023; Mafei *et al.*, 2020).

2.5.5. UV-Visible spectral scanning

Filtered aliquots (0.45 µm) were analyzed using a Thermo Scientific Genesys 10S UV-Visible spectrophotometer. Spectra were recorded over 190–700 nm to assess the presence of chromophoric and aromatic compounds.

2.6. Characterization of activated carbon

2.6.1. Contact pH

The contact pH of the commercial AC was determined following ASTM D6851-20 with minor modifications (Astm International, 2020). One gram of dried

AC was mixed with 10 mL of deionized water and stirred at 25 ± 2 °C for 30 min to reach equilibrium. The pH of the supernatant was measured using a calibrated pH meter (buffers pH 4.0, 7.0, and 10.0). The resulting value represents the carbon's contact pH, reflecting its tendency to modify the aqueous medium.

2.6.2. Fourier transform Infrared attenuated total reflectance spectroscopy (FTIR-ATR)

Surface functional groups of AC were identified by FTIR-ATR using a Bruker ALPHA spectrometer. Dried samples were analyzed directly in the sample holder over 4000–400 cm^{-1}, with 4 cm^{-1} resolution and 32 scans. Bands were assigned to specific functional groups (O–H, C=O, C–O, C=C) following Ali et al. (2020) (Ali *et al.*, 2025).

2.6.3. X-ray diffraction (XRD)

Crystallinity and structural order of AC were examined by X-ray diffraction using a Shimadzu XRD-6000 diffractometer (Cu-Kα, λ = 1.5406 Å), operated at 40 kV and 30 mA. Patterns were collected between 10° and 80° (2θ) at a scan rate of 2° min^{-1}. Diffractograms were interpreted based on the presence of graphite-like (002) and (100) reflections (Astm International, 2020).

2.6.4. Scanning Electron Microscopy (SEM) and Energy-Dispersive X-ray Spectroscopy (EDX)

Morphological analysis was performed using a Zeiss EVO 10 MA scanning electron microscope operated at 20 kV, with magnifications of 1.0 k× and 5.0 k×. Samples were mounted on carbon adhesive stubs and gold-coated (≈ 75 nm) before imaging (De Souza Silv *et al.*, 2021).

3. RESULTS AND DISCUSSION

3.1. Characterization of activated carbon

The contact pH of the commercial AC was 9.9, whereas deionized water presented a pH of 6.9. This result indicates that the AC has an alkaline surface nature and tends to increase the pH of aqueous solutions. Similar findings were

reported by Finn et al. (2021), who evaluated various commercial activated carbons for pharmaceutical removal at the point-of-entry and found contact pH values ranging from 3.2 to 11.8, depending on the precursor material and activation type (Finn *et al.*, 2021). Bituminous-based carbons exhibited contact pH around 9.8, while coconut-based carbons reached values of approximately 10.9–11.3. Likewise, Vojnović et al. (2022) investigated the influence of initial pH on the adsorption of Reactive Black 5 dye using powdered activated carbon and demonstrated that adsorption remained highly effective across acidic and alkaline media (Vojnovic *et al.*, 2022). These results confirm that alkaline carbons can maintain high adsorption efficiency even at elevated pH, highlighting the importance of characterizing the contact pH prior to application. The observed alkalinity is attributed to basic surface groups such as hydroxyl and carbonate functionalities capable of releasing hydroxide ions (OH^-) in water, increasing solution alkalinity. This parameter is relevant in adsorption processes because it affects the surface charge of the adsorbent and therefore its affinity toward ionic or polar species. Carbons with high contact pH values are generally more effective in adsorbing anionic compounds at pH above their point of zero charge (pH_PZC).

Figure S1 from **ESI** shows the ATR-FTIR spectrum, which exhibits absorption bands in the 3800–2400 and 1500 cm^{-1} regions. The band at ~1500 cm^{-1} is the most relevant, corresponding to the aromatic C=C stretching vibration, characteristic of the graphitic structure of the material. This band represents the only absorption directly associated with the carbonaceous matrix and indicates a high degree of carbonization. This observation is consistent with Rizwan et al. (2020), who reported that untreated charcoal displays only weak peaks at ~1632 cm^{-1} attributed to minor fractions of conjugated C=O groups, while predominantly exhibiting aromatic carbon domains. The signals observed at ~3800 cm^{-1} and ~2400 cm^{-1} correspond to atmospheric water vapor and CO_2 absorption, respectively, commonly reported in FTIR spectra of carbon-based materials, and are not intrinsic to the charcoal surface (24).

Figure 1 presented the XRD pattern exhibited intense peaks near 22° and 26° (2θ), corresponding to the (002) and (100) graphite planes, respectively. These reflections indicate the presence of ordered graphitic domains and

moderate crystallinity within the carbon matrix. According to Malini et al. (2023), sharper and more intense peaks correspond to a higher degree of structural ordering in carbonaceous materials (Malini; Selvakumar; Kumar, 2023). Therefore, the obtained diffractogram suggests that the activated carbon possesses semi-crystalline domains, which may enhance its adsorption performance by providing both micro- and mesoporous structures.

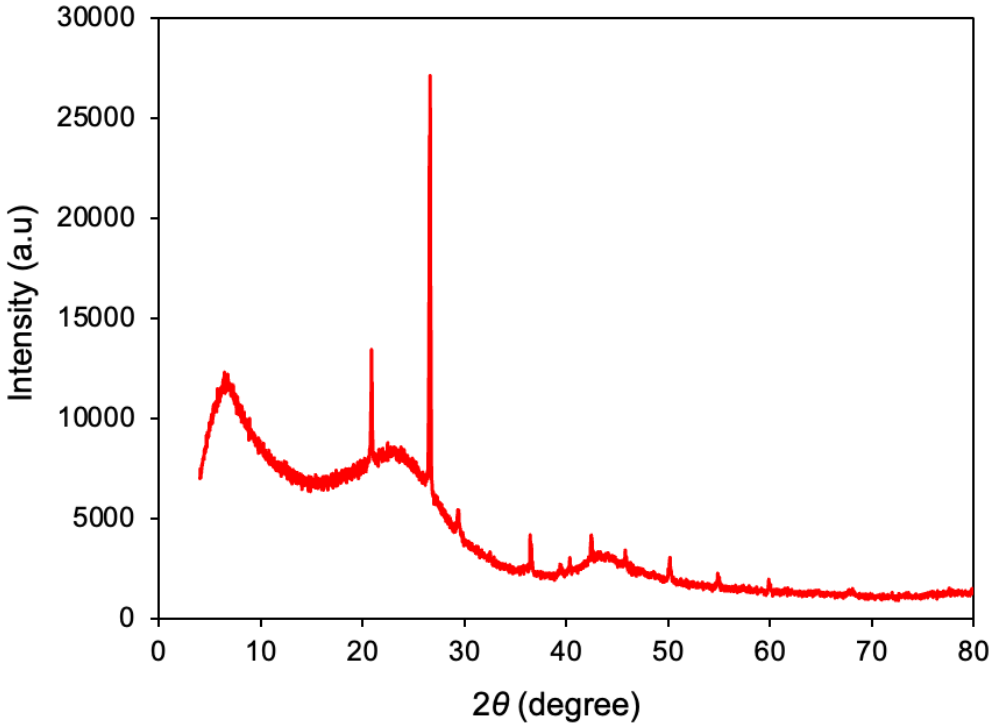

Figure 1. X-ray diffraction (XRD) patterns of activated carbon (AC).

Figure 2 presented SEM micrographs revealed that the AC possesses a highly heterogeneous morphology, comprising irregular fragments, lamellar structures, and porous surfaces. Layered regions coexisted with rougher, fractured zones, highlighting its substantial porosity. This complex structure provides a large surface area and an intricate pore network, which enhances the adsorption of organic molecules and ions, supporting its effectiveness for hydrolysate purification. Low-magnification images (1000x) displayed the overall irregular and non-uniform morphology, with a mixture of flake-like and fragmented particles typical of commercial activated carbon. Higher-magnification views (5000x) revealed fine surface details, including plate-like fragments, sharp edges,

and small particles or debris adhering to surfaces. Certain regions exhibited layered, sheet-like arrangements with parallel grooves, suggesting graphitic-like structures. Together, these features indicate a combination of high surface area and accessible porosity, confirming the AC´s suitability for efficient adsorption.

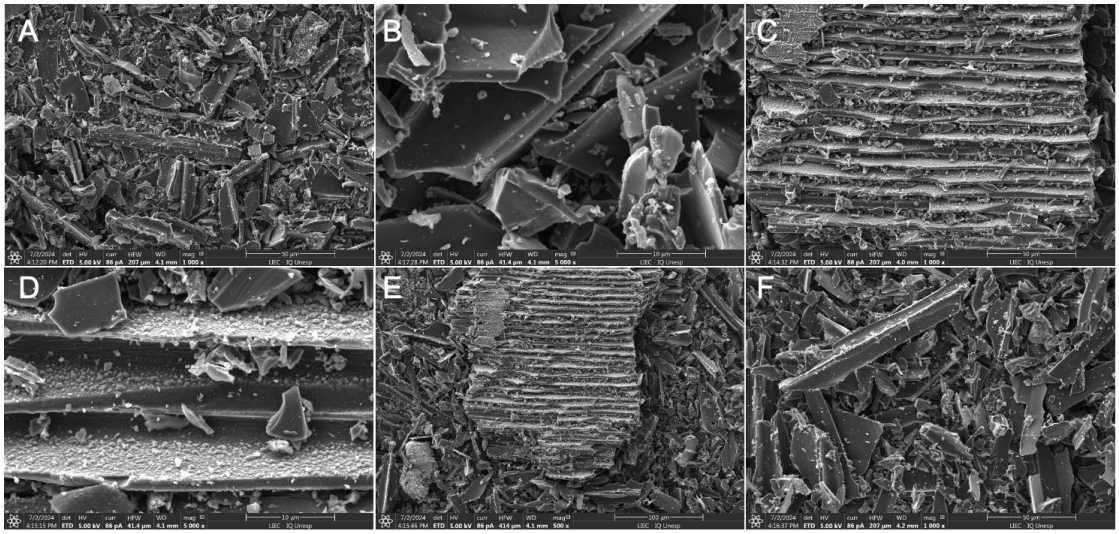

Figure 2. Scanning electron microscopy (SEM) images of activated carbon (AC), illustrating its surface morphology and porous structure. Images were acquired at magnifications of (e) 500x, (a, c, f) 1000x and (b, d) 5000x.

3.2. Adsorption of target and inhibitory compounds

The adsorption performance of AC toward representative groups of compounds presents in lignocellulosic hydrolysates revealed a clear pattern of chemical selectivity (**Figure 3**). The adsorption of XOS (**Figure 3A**) decreased progressively with the degree of polymerization. Xylobiose and xylotriose showed moderate adsorption efficiencies, ranging from 35 to 50%, while xylotetraose and higher oligomers (XOS>6) exhibited much lower adsorption (15-30%). This inverse relationship between molecular size and adsorption capacity suggests that diffusion and steric effects play a dominant role. In fact, smaller XOS molecules can access mesopores and interact with internal surface sites, whereas larger oligomers experience restricted diffusion and steric hindrance. Moreover, the abundance of hydroxyl groups in these oligosaccharides enhances their hydrophilicity, weakening their interaction with the predominantly hydrophobic surface of activated carbon (Zeng; Van Pijkeren; Pan, 2023).

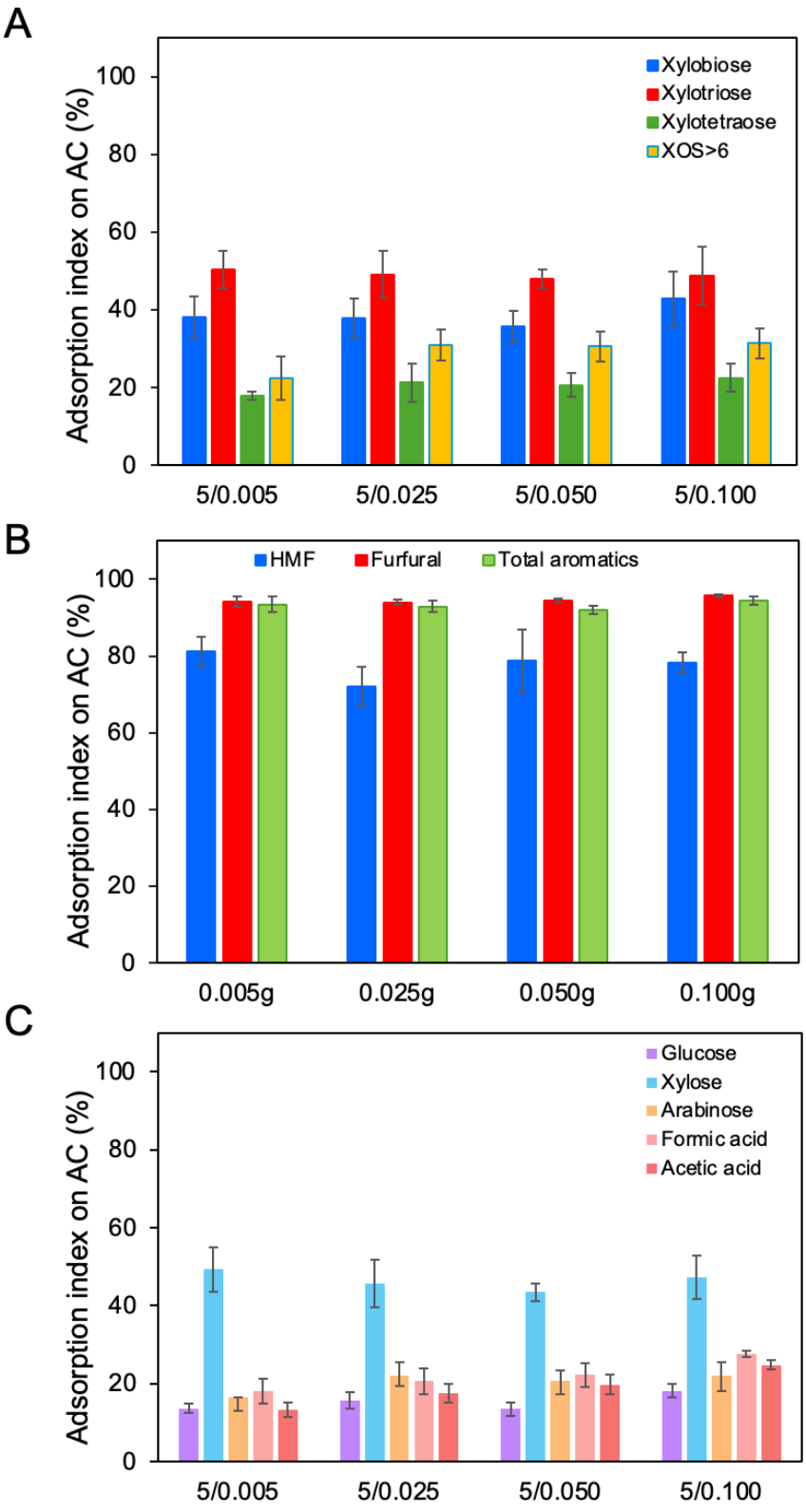

Figure 3. (A) Adsorption index of xylooligosaccharides (XOS) on activated carbon (AC) at different adsorbent ratios. (B) Adsorption index of furanic (furfural and hydroxymethylfurfural, HMF) and total aromatics compounds on activated carbon (AC) at different adsorbent ratios. (C) Adsorption index of sugars and organic acids on activated carbon at different adsorbent ratios.

In contrast, strong adsorption was observed for aromatic and furanic compounds (**Figure 3B**). Furfural and total aromatics were almost completely removed from the liquid phase, with adsorption indices exceeding 90%, while HMF displayed slightly lower but still substantial adsorption values (70-85%). These results confirm the high affinity of AC for conjugated molecules, which is mainly governed by π–π stacking interactions and hydrophobic forces between the aromatic carbon surface and the electron-rich π systems of furans and total aromatics. Such strong retention of inhibitory compounds has been consistently reported in lignocellulosic hydrolysate detoxification, where activated carbon preferentially removes furans and phenolics while preserving fermentable sugars (Tavares *et al.*, 2022). Monosaccharides and low-molecular-weight organic acids displayed distinct adsorption behaviors on activated carbon (**Figure 3C**). Glucose and arabinose were only weakly adsorbed, with removal rates below 20%, whereas xylose showed a markedly higher adsorption index, exceeding 50%. Formic and acetic acids also exhibited very low adsorption (<20%), consistent with their high polarity and complete miscibility in water. The unexpectedly higher adsorption of xylose may be related to its intermediate polarity and smaller molecular size, which could facilitate its diffusion into the mesoporous structure of the activated carbon. In addition, hydrogen bonding between xylose hydroxyl groups and oxygen-containing surface functionalities on the carbon (e.g., carbonyl or phenolic sites) may enhance its retention compared to other monosaccharides. The limited adsorption of glucose, arabinose, and organic acids can be attributed to their strong solvation and hydrophilicity, which favor interactions with the aqueous phase rather than with the hydrophobic carbon surface. The presence of multiple hydroxyl or carboxyl groups increases their affinity for polar solvents, therefore reducing their tendency to adsorb onto the carbon matrix.

Indeed, these results highlight the strong adsorptive selectivity of AC toward total aromatics and furanic compounds over carbohydrates and acids. The mechanism involves preferential adsorption of less polar, planar molecules through π–π interactions and van der Waals forces, while polar and bulky species are excluded by steric and solvation effects. For oligosaccharides, the adsorption

process is additionally governed by molecular size and the accessibility of pores within the carbon structure. This selective behavior aligns with previous findings reported by Montané et al. (2006), who demonstrated that the pore size distribution and surface chemistry of carbon materials are key parameters controlling the selective retention of oligosaccharides and aromatic compounds during hydrolysate purification (Montané *et al.*, 2006).

3.3. Desorption and recovery of compounds

To assess compound recovery and evaluate the potential reusability of AC, desorption experiments were carried out using solvents of increasing polarity (H_2O, 15%, 30%, and 50% ethanol). **Figures 4A-C** show the desorption indices obtained for XOS, monosaccharides and organic acids, and furanic/aromatic compounds, respectively.

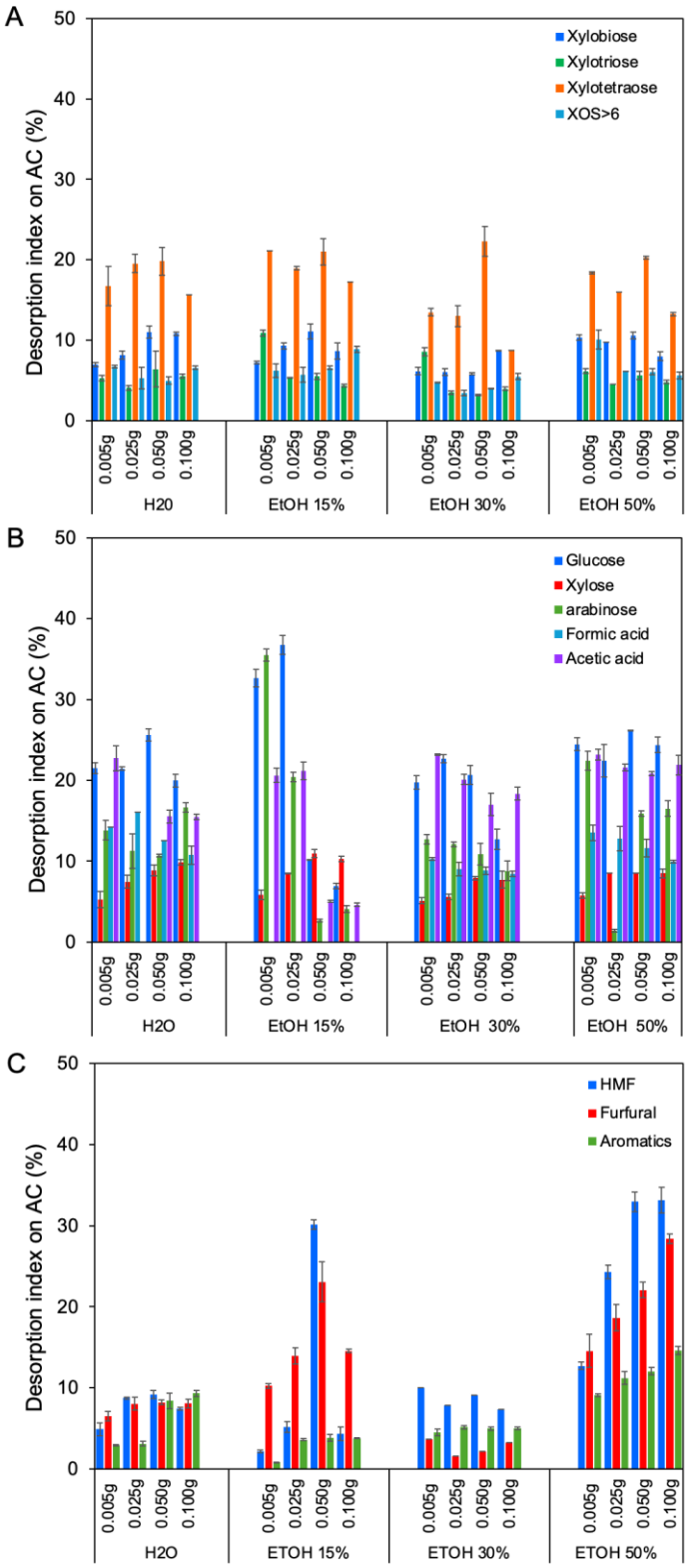

Figure 4. Desorption behavior of different hydrolysate components from activated carbon (AC) using water and ethanol-water mixtures (15, 30, and 50% v/v). (A) Xylooligosaccharides (XOS) with different degrees of polymerization. (B) Monosaccharides and organic acids. (C) Furanic (furfural and hydroxymethylfurfural, HMF) and total aromatics compounds.

Among the XOS fractions (**Figure 4A**), xylotetraose consistently exhibited the highest desorption indices (15-25%), particularly when 30% ethanol was used. This suggests that ethanol-water mixtures of intermediate polarity enhance the solubilization of these partially hydrophilic molecules by weakening hydrogen bonds between hydroxyl groups and the carbon surface. Lower molecular weight oligomers, such as xylobiose and xylotriose, showed limited recovery (<15%), which is consistent with their weaker adsorption affinity and faster desorption equilibrium. The desorption of highly polymerized fractions (XOS>6) remained low (<10%), indicating that steric hindrance and restricted pore accessibility still limit solvent penetration and elution efficiency. Increasing the AC mass from 0.005 to 0.050 g improved desorption slightly, suggesting a balance between available surface sites and solvent-solute competition; however, above 0.050 g no further enhancement was observed, indicating equilibrium saturation. These findings align with previous reports showing that moderate ethanol concentrations (20-40%) favor the selective recovery of oligosaccharides without co-eluting strongly adsorbed aromatic inhibitors (Zhang *et al.*, 2018). Furthermore, the desorption behavior of monosaccharides and organic acids was strongly dependent on solvent polarity (**Figure 4B**). Overall, desorption increased with ethanol concentration, confirming that mixed solvents enhance recovery compared to pure water. The highest recoveries (20-35%) were observed for glucose and arabinose in 15-30% ethanol, while xylose showed comparatively lower release, consistent with its stronger adsorption affinity observed earlier (*previous section*). Formic and acetic acids were moderately desorbed (10-25%) in ethanol-water mixtures, particularly at higher ethanol concentrations, reflecting improved solubilization of these small polar molecules. In pure water, all compounds exhibited poor desorption (<15%), indicating that highly polar solvents cannot efficiently disrupt solute-surface interactions. The observed increase with ethanol concentration suggests that the weakening of hydrogen bonding and enhanced solvent penetration within pores play key roles in desorption dynamics. Concerning, furanic and total aromatics compounds displayed markedly different desorption profiles compared to sugars (**Figure 4C**). HMF and furfural showed the highest recoveries in 15-50% ethanol, reaching up

to 30-35% for HMF, whereas water alone resulted in negligible desorption (<10%). This trend highlights the greater efficiency of less polar solvents in breaking hydrophobic and π–π interactions between furanic compounds and the graphitic surface of AC. Conversely, total aromatics compounds exhibited low desorption (<15%) under all solvent conditions, suggesting stronger, irreversible π–π stacking interactions that are not easily disrupted by ethanol at the tested concentrations. These results indicate that while moderate ethanol mixtures can release a portion of adsorbed furans, total aromatics inhibitors remain more tightly bound to the carbon surface, possibly requiring higher ethanol content or alternative desorbing agents for complete recovery.

It's important to highlight that the combined results demonstrate a clear relationship between solvent polarity and compound recovery. Ethanol-water mixtures of intermediate polarity (15-30%) achieved the best balance, efficiently desorbing moderately polar compounds such as oligosaccharides and furans, while maintaining selective retention of strongly adsorbed total aromatics. The efficiency plateau observed with increasing AC dosage suggests that desorption is governed by equilibrium processes involving both solute-surface affinity and solvent-solute interactions. These findings reinforce the concept that controlled solvent polarity is essential to optimize both detoxification and product recovery from lignocellulosic hydrolysates, in agreement with earlier studies by Zhang et al. (2018) and related reports on carbon-based purification systems (Zhang *et al.*, 2018).

3.4. Selective purification of HH by AC treatment

Table 1 summarizes the composition of the hemicellulosic hydrolysate (HH) after vacuum evaporation and subsequent treatment with increasing doses of AC. The main objective was to assess the selectivity and efficiency of AC in removing undesirable compounds while preserving the target XOS.

Table 1. Concentration of desirable and undesirable compounds in the hemicellulosic hydrolysate (HH) after vacuum evaporation, including the concentration factor of each component and the respective removal rates or losses observed after treatment with AC.

	Post- evaporation (g.L-1)	0.005g (g.L-1)	0.025g (g.L-1)	0.050g (g.L-1)	0.100g (g.L-1)
Target-compounds (g.L-1)					
Xylobiose	12.48±2.07	8.18±0.68	8.27±1.01	8.35±0.49	7.66±0.91
Xylotriose	7.58±1.35	5.59±0.63	5.56±0.77	5.79±0.26	5.79±0.58
Xylotetraose	6.68±0.02	5.61±0.12	5.34±0.39	5.59±0.21	5.38±0.24
XOS>6	84.79±2.00	66.83±5.35	60.97±6.33	60.45±3.25	60.45±3.25
Total	111.54	86.21	80.14	80.19	79.28
Unwanted compounds (g.L-1)					
Total aromatics	14.43±0.35	0.94±0.32	1.08±0.21	1.20±0.19	0.76±0.14
Xylose	22.62±3.38	13.90±1.63	15.21±1.76	15.78±0.58	14.62±1.53
Furfural	0.08±0.00020	0.006±0.001	0.005±0.001	0.005±0.0005	0.004±0.000
HMF	0.34±0.0011	0.08±0.01	0.10±0.01	0.10±0.01	0.09±0.01
Acetic Acid	5.15±0.09	4.63±0.05	4.41±0.07	4.35±0.35	4.04±0.09
Glucose	2.71±0.48	2.43±0.05	2.39±0.04	2.33±0.05	2.33±0.05
Arabinose	3.08±0.44	2.66±0.10	2.01±0.31	2.52±0.31	2.52±0.12
Formic Acid	2.35±0.25	1.95±0.17	1.91±0.17	1.89±0.08	1.77±0.02
Total	50.76	26.59	27.11	28.19	26.14
Purification index (%)	68.73	76.43	74.72	73.99	75.20

After concentration by vacuum evaporation, the HH exhibited a high XOS content (111.5 gL^{-1}), predominantly composed of higher-degree oligomers (XOS >6). Subsequent AC treatment led to a moderate decrease in total XOS concentration to approximately 79 gL^{-1}, corresponding to a 30% loss. The largest reductions were observed in high-molecular-weight fractions, likely due to partial adsorption through hydrophobic and van der Waals interactions with the carbon surface, whereas lower-degree oligomers (xylobiose, xylotriose, and xylotetraose) showed smaller decreases, indicating a selective adsorption pattern in which AC preferentially binds non-polar inhibitors rather than hydrophilic sugars. This selectivity aligns with the high polarity and aqueous solubility of XOS, which favor strong solvation and weak affinity toward the hydrophobic carbon matrix. AC treatment also resulted in a marked reduction of inhibitory compounds, confirming its strong adsorptive capacity. Total aromatics decreased drastically from 14.43 gL^{-1} to 0.76-1.2 gL^{-1} (>90% removal), attributed to π–π stacking interactions between aromatic rings and the graphitic carbon surface, while furfural and HMF, both hydrophobic furan derivatives, were almost completely eliminated (<0.01 gL^{-1}) through nonpolar adsorption in micropores. In contrast, organic acids (acetic and formic) and monosaccharides (glucose, xylose, and arabinose) showed only minor decreases (10-25%), consistent with their high polarity and low affinity for the carbon surface. These contrasting behaviors demonstrate a selective adsorption mechanism governed by molecular polarity, size, and π–π interaction potential. The purification index, representing the relative increase in the XOS-to-impurities ratio, ranged from 68.7% to 75.2%, with no significant improvement observed beyond 0.025 g of AC, suggesting surface saturation at higher dosages and indicating that small amounts of AC suffice to achieve maximum purification efficiency, which highlights the economic and scalable potential of the process. Compared with ethyl acetate extraction reported by Otaviano et al. (2023), AC achieved similar purification efficiency (~75%) while offering advantages such as lower XOS loss, absence of residual organic solvents, and reduced environmental impact, positioning AC treatment as a green and cost-effective alternative for HH purification (Otaviano *et al.*, 2023). Mechanistically, the adsorption behavior supports a selectivity model based on physicochemical properties: hydrophobic inhibitors are strongly retained via π–π and dispersion interactions, whereas hydrophilic carbohydrates

remain largely unabsorbed due to solvation effects and weak hydrophobic interactions. Subsequent ethanol-water desorption allows differential recovery, with 30% ethanol selectively eluting XOS and 50% ethanol efficiently removing furanic wastes. Overall, these results confirm that AC is an efficient, selective, and environmentally friendly adsorbent for the purification of XOS-rich HH of *Eucalyptus* by-products. AC selectively removed hydrophobic inhibitors while preserving most of the XOS fraction, achieving a high purification index (≈75%) with moderate XOS losses, demonstrating its potential as a sustainable and low-impact purification step for biotechnological applications of XOS.

4. CONCLUSION

This study demonstrated that AC is an effective and sustainable adsorbent for purifying XOS from HH of *Eucalyptus* byproduct. Its alkaline, graphitic, and porous surface favored selective adsorption of hydrophobic inhibitors, achieving >90% removal of furfural, HMF, and total aromatics while preserving most XOS. Adsorption selectivity was governed by molecular polarity and size, and ethanol-water desorption allowed selective recovery of XOS (30% ethanol) and furanic/aromatic compounds (50% ethanol). The purification index reached 68.7-75.2%, comparable to solvent-based methods but with lower complexity and environmental impact. These findings highlight AC as a simple, low-cost, and environmentally friendly option for scalable XOS purification, with future work needed to optimize conditions and evaluate adsorbent reuse for industrial applications.

Abbreviations

XOS	Xylooligosaccharides
AC	Activated Carbon
HH	Hemicellulosic Hydrolysate
HMF	Hydroxymethylfurfural
SCFA	Short-Chain Fatty Acids
HPLC	High-Performance Liquid Chromatography
UV-Vis	Ultraviolet–Visible Spectrophotometry

Abbreviations

FTIR-ATR	Fourier Transform Infrared – Attenuated Total Reflectance
XRD	X-ray Diffraction
SEM	Scanning Electron Microscopy
EDX	Energy-Dispersive X-ray Spectroscopy
ODS	Octadecylsilane (C18) column
ASTM	American Society for Testing and Materials
RID	Refractive Index Detector
DP	Degree of Polymerization
P_2O_5	Phosphorus Pentoxide
pH_PZC	Point of Zero Charge

5. REFERENCES

CARVALHO, A. F. A. et al. M. Xylo-oligosaccharides from lignocellulosic materials: Chemical structure, health benefits and production by chemical and enzymatic hydrolysis. ***Food Research International***, v. 51, p. 75–85, 2013.

MOURE, A. et al. Advances in the manufacture, purification and applications of xylo-oligosaccharides as food additives and nutraceuticals. ***Process Biochemistry***, v. 41, p. 1913–1923, 2006.

XU, J. et al. Use of xylooligosaccharides (XOS) in hemicelluloses/chitosan-based films reinforced by cellulose nanofiber: Effect on physicochemical properties. ***Food Chemistry***, v. 298, 2019.

ANTOV, M. G.; ĐORĐEVIĆ, T. R. Environmental-friendly technologies for the production of antioxidant xylooligosaccharides from wheat chaff. ***Food Chemistry***, v. 235, p. 175–180, 2017.

ZHANG, X. et al. Coproduction of xylooligosaccharides and fermentable sugars from sugarcane bagasse by seawater hydrothermal pretreatment. ***Bioresource Technology***, v. 309, 2020.

MANICARDI, T. et al. Xylooligosaccharides: A bibliometric analysis and current advances of this bioactive food chemical as a potential product in biorefineries' portfolios. ***Foods***, v. 12, 2023.

VÁZQUEZ, M. J. et al. Manufacture and applications. Production of xylooligosaccharides from lignocellulosic materials, 2000.

IBÁ – INDÚSTRIA BRASILEIRA DE ÁRVORES. *Relatório anual 2024*. São Paulo, 2024. Disponível em: https://iba.org/datafiles/publicacoes/relatorios/relatorio-iba-2024.pdf. Acesso em: 17 set. 2025.

DA SILVA, A. A. et al. Caracterização das O-acetil-(4-O-metilglicurono)xilanas isoladas da madeira de *Eucalyptus urograndis*. ***Química Nova***, v. 31, 2008.

SAMANTA, A. K. et al. Xylooligosaccharides as prebiotics from agricultural by-products: Production and applications**.** ***Bioactive Carbohydrates and Dietary Fibre***, v. 5, p. 62–71, 2015.

FUTURE MARKET INSIGHTS INC. Xylooligosaccharide market expected to grow at 7% CAGR and surpass US$ 144.5 million by 2033. *AccessNewswire*, 2023. Disponível em: https://www.accessnewswire.com/newsroom/en/business-and-professional-services/xylooligosaccharide-market-expected-to-grow-at-7-cagr-and-surpass-750911. Acesso em: 17 set. 2025.

TAMAYO-PEÑA, J. A. et al. Eucalyptus grandis forestry residue valorization: Distinct and integrated pretreatment methods for enhanced xylooligosaccharide production**.** ***Bioenergy Research***, v. 17, n. 3, p. 1503–1521, 2024.

NOBRE, C.; TEIXEIRA, J. A.; RODRIGUES, L. R. Fructo-oligosaccharides purification from a fermentative broth using an activated charcoal column. ***New Biotechnology***, v. 29, n. 3, p. 395–401, 2012.

ZHU, J. et al. A green process for producing xylooligosaccharides from poplar: Endoxylanase assisted autohydrolysis, activated carbon separation, and spent liquor for rice growth. ***Industrial Crops and Products***, v. 174, 2021.

OTAVIANO, A. C. A. et al. Hydrothermal pretreatment of eucalyptus by-product and refining of xylooligosaccharides from hemicellulosic hydrolysate. ***Separation and Purification Technology***, v. 306, 2023.

PASCHOA, J. L. F. et al. Production and purification of xylooligosaccharides from sugarcane bagasse and antioxidant potential assessment for functional ingredient application in the food industry**.** ***Industrial Crops and Products***, v. 208, 2024.

ZHANG, J. et al. Investigating desorption during ethanol elution to improve the quality and antioxidant activity of xylo-oligosaccharides from corn stalk. ***Bioresource Technology***, v. 249, p. 342–347, 2018.

MAFEI, T. D. T. et al. Extraction and characterization of hemicellulose from eucalyptus by-product: Assessment of enzymatic hydrolysis to produce xylooligosaccharides. ***Applied Biochemistry and Biotechnology***, v. 190, n. 1, p. 197–217, 2020.

ASTM INTERNATIONAL. *Test method for determination of contact pH with activated carbon*. **West Conshohocken**, 2020. Disponível em: http://www.astm.org/cgi-bin/resolver.cgi?D6851-20. Acesso em: 17 set. 2025.

ALI, K. et al. Xylooligosaccharides: A comprehensive review of production, purification, characterization, and quantification. ***Food Research International***, v. 201, 2025.

DE SOUZA SILVA, A. P. et al. Inajá oil processing by-product: A novel source of bioactive catechins and procyanidins from a Brazilian native fruit. ***Food Research International***, v. 144, 2021.

FINN, M. et al. Activated carbon for pharmaceutical removal at point-of-entry. ***Processes***, v. 9, n. 7, 2021.

VOJNOVIĆ, B. et al. Influence of initial pH value on the adsorption of Reactive Black 5 dye on powdered activated carbon: Kinetics, mechanisms, and thermodynamics. ***Molecules***, v. 27, n. 4, 2022

ALI, R. et al. BET, FTIR, and RAMAN characterizations of activated carbon from waste oil fly ash. ***Turkish Journal of Chemistry***, v. 44, n. 2, p. 279–295, 2020.

MALINI, K.; SELVAKUMAR, D.; KUMAR, N. S. Activated carbon from biomass: Preparation, factors improving basicity and surface properties for enhanced CO_2 capture capacity – A review. ***Journal of CO_2 Utilization***, v. 67, 2023.

ZENG, M.; VAN PIJKEREN, J.; PAN, X. Gluco-oligosaccharides as potential prebiotics: Synthesis, purification, structural characterization, and evaluation of prebiotic effect. ***Comprehensive Reviews in Food Science and Food Safety***, v. 22, n. 4, p. 2611–2651, 2023.

TAVARES, A. P. M. et al. Cardoon hydrolysate detoxification by activated carbon or membranes system for bioethanol production. ***Energies***, v. 15, n. 6, p. 1993, 2022.

MONTANÉ, D. et al. Removal of lignin and associated impurities from xylo-oligosaccharides by activated carbon adsorption. ***Industrial & Engineering Chemistry Research***, v. 45, n. 7, p. 2294–2302, 2006.

6. MATERIAL SUPPLEMENTARY

ELECTRONIC SUPPLEMENTARY INFORMATION (ESI)

Purification of xylooligosaccharides from *Eucalyptus* by-product using activated carbon adsorption

Cecília Aline Otaviano,[1] Cassamo Ussemane Mussagy,[2] Fernando Masarin,[1*]

[1]São Paulo State University (UNESP), School of Pharmaceutical Science (FCF), Department of Bioprocess Engineering and Biotechnology. Araraquara-SP, Brazil. 14800-903

[2]Laboratorio de Desarrollo de Bioprocesos Sostenibles (Labisost), Escuela de Agronomía, Facultad de Ciencias Agronómicas y de los Alimentos, Pontificia Universidad Católica de Valparaíso, Casilla 4-D, Quillota 2260000, Chile.

(*) Corresponding author: fernando.masarin@unesp.br

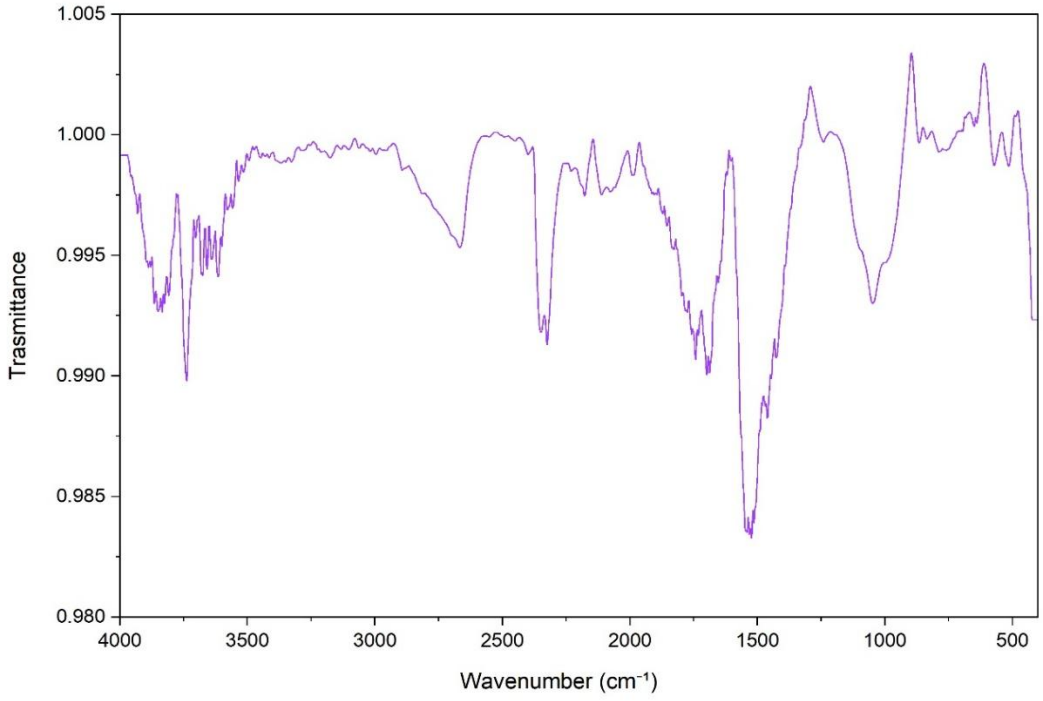

Figure 1. Fourier transform Infrared attenuated total reflectance spectroscopy (ATR-FTIR) spectra of activated carbon (AC).

3 CHAPTER II

Xylooligosaccharides obtained from the hydrothermal pretreatment of *Eucalyptus* by-product as functional ingredients with dual function: potential prebiotic and antioxidant properties

[1]Cecília Aline Otaviano, [2]Omar David Pino Vargas, [2]Nathalia Correa Guzmán, [2]Julián Paul Martínez Galán, [3]Mateus Kawata Salgaço, [3]Kátia Sivieri, [4]Elias de Souza Monteiro Filho, [3]Flavia Aparecida Resende Nogueira, [1*]Fernando Masarin[*]

[1]São Paulo State University (UNESP), School of Pharmaceutical Science (FCF), Department of Bioprocess Engineering and Biotechnology. Araraquara-SP, Brazil. 14800-903

[2]University of Antioquia (UdeA), School of Nutrition and Dietetic, Medellin, Colombia, Calle 62 # 52 - 59, 050010

[3]University of Araraquara (UNIARA), Araraquara-SP, Brazil 14801-320

[4]Institute of Chemistry, São Paulo State University (UNESP), Araraquara, SP, Brazil 14800-060

(*) Corresponding author

Email addresses:
CAO: cecilia.otaviano@unesp.br
OMPV: omar.pino@udea.edu.co
NCG: nathalia.correag@udea.edu.co
JPMG: julian.martinez@udea.edu.co
KS: katia.sivieri@unesp.br
MKS: mateus.salgaco@unesp.br
EMF: elias.monteiro@unesp.br
FARN: farnogueira@uniara.edu.br
FM: fernando.masarin@unesp.br

ABSTRACT

The use of lignocellulosic byproducts to obtain functional ingredients has gained prominence in the context of the circular bioeconomy. Xylooligosaccharides (XOS), produced from the hemicellulosic fraction of *Eucalyptus* by hydrothermal pretreatment (HP) and purification, have recognized prebiotic properties and potential antioxidant activity. In this study, the in vitro functional effect of an XOS-extract was evaluated, considering its impact on the growth of *Lactobacillus acidophilus* and *Lacticaseibacillus rhamnosus*, its influence on in vitro batch fermentation, on the composition of the intestinal microbiota, and on antioxidant activity, determined by the DPPH and FRAP methods. Cytotoxicity was evaluated in Caco-2 cells by the resazurin assay. The XOS-extract promoted a significant increase in the growth of probiotic strains in glucose-free MRS medium, although with a lower effect than that observed for inulin. In colonic simulation assays, an increase in the production of acetic acid and total short-chain fatty acids (SCFA) was observed at the intermediate and higher doses, furthermore to a partial reduction in ammonia levels, suggesting modulation of microbial metabolism towards a predominantly saccharolytic profile. Nevertheless, the prebiotic index (PI) remained negative at all doses, indicating that the selective effects were discreet, possibly due to the presence of residual compounds in the XOS-extract. Regarding antioxidant activity, the extract showed significant radical scavenging capacity, with EC_{50} values of 44.13 μg·mL^{-1} (DPPH) and 188.57 μg·mL^{-1} (FRAP). Cytotoxicity was considered low, with an IC_{50} in Caco-2 cells of approximately 1.497 μg·mL^{-1}. In general, XOS-extract derived from *Eucalyptus* byproducts demonstrate potential as a dual-action functional ingredient, combining prebiotic activity in isolated cultures and relevant antioxidant properties. However, further studies are needed to optimize XOS-extract purity and validate effects in more complex biological models.

Keywords: xylooligosaccharides; antioxidant capacity; microbial modulation.

1. INTRODUCTION

The human gastrointestinal tract harbors a complex and dynamic microbial community, composed of trillions of microorganisms that play essential roles in maintaining homeostasis and promoting host health (Sender; Fuchs; Milo, 2016; Thursby; Juge, 2017). This gut microbiota plays a role in fundamental physiological processes, such as digestion and absorption of nutrients, vitamin synthesis, immune system maturation, and protection against pathogenic microorganisms (Alvarez; Fernández0; Ciancia, 2024; Valladares-Diestra *et al.*, 2023). Alterations in this balance, known as dysbiosis, are associated with metabolic and inflammatory disorders, including obesity, metabolic syndrome, inflammatory bowel diseases, and alterations in the gut-brain axis (Thusby; Juge, 2017).

Among the strategies investigated to favorably modulate this microbiota, prebiotics, probiotics, and symbiotics stand out, with prebiotics being widely recognized for selectively stimulating the growth of beneficial bacterial populations, especially Lactobacillus and Bifidobacterium, promoting health benefits for the host (Gibson, Glenn *et al.*, 2017; Markowiak; Ślizewska, 2017). Prebiotics are defined as non-digestible food ingredients that, through selective fermentation in the colon, produce short-chain fatty acids (SCFAs) such as acetate, propionate, and butyrate, metabolites with positive effects on lipid metabolism, intestinal mucosal integrity, and immune modulation (Gibson, Glenn. *et al.*, 2017; Rycroft *et al.*, 2001; Slavin, 2013).

Among the main prebiotics studied are fructooligosaccharides (FOS), galactooligosaccharides (GOS), and xylooligosaccharides (XOS), which differ from each other in their monosaccharide composition and the predominant type of glycosidic linkage (Palaniappan; Antony; Emmambux, 2021; Rycroft *et al.*, 2001). XOS consist of oligomers of 2 to 10 xylose units linked by β-(1,4) type bonds, formed from the controlled hydrolysis of the xylan fraction, one of the main polysaccharides present in lignocellulosic biomass, such as in hardwoods and grasses, as well as their derivatives (Henriques *et al.*, 2023; Palaniappan; Antony; Emmambux, 2021).

Due to their low caloric value, high thermal and chemical stability, and fermentative selectivity, XOS are emerging as promising functional ingredients for application in food and supplements, without compromising sensory or

nutritional properties (Míguez *et al.*, 2021; Palanippan; Antony; Emmambux, 2021; Samanta *et al.*, 2015). Recent studies demonstrate that XOS selectively promote the growth of Lactobacillus and Bifidobacterium, associated with improved intestinal barrier function, enhanced immune response, and reduced inflammation (Alvarez; Fernández; Ciancia, 2024; Finegold *et al.*, 2014; Lin *et al.*, 2016; Samanta *et al.*, 2015). The fermentation of these compounds results in the production of SCFAs that reduce intestinal pH and promote an environment conducive to the colonization of beneficial microorganisms (Lin et al., 2016).

The sustainable production of XOS has attracted scientific and industrial attention in the context of circular bioeconomy and the valorization of lignocellulosic by-products. Agro-industrial by-products such as sugarcane bagasse, cereal straw, and by-products from the pulp and paper industry have a high xylan content, making them promising substrates for XOS production via hydrothermal, chemical, or enzymatic processes (Henriques *et al.*, 2023; Palaniappan; Antony; Emmambux, 2021). Among these sources, *Eucalyptus* stands out as one of the most abundant raw materials in Brazil. *Eucalyptus* by-product, rich in xylan, represents sustainable and technically viable alternatives for obtaining XOS, a high value-added product (Otaviano et al., 2023; Paz-Cedeno, 2022).

Therefore to prebiotic activity, *Eucalyptus*-derived XOS exhibit antioxidant activity, contributing to the prevention of oxidative damage at the cellular level. (George *et al.*, 2022; Li, Wei *et al.*, 2020; Putpadungwinpon; Powthong, 2025). This property can be evaluated by in vitro assays, which allow quantifying the antioxidant activity of the XOS-rich extract (Putpadungwipon; Powthong, 2025).

For microbiological studies, Man, Rogosa and Sharpe (MRS) culture medium is widely used for the cultivation of lactic acid bacteria, especially Lactobacillus, and has been employed in evaluating the prebiotic activity of XOS (Charteris *et al.*, 1998; Corcoran *et al.*, 2005; Gibson; Roberfroid, 1995). Its composition promotes microbial growth and can be modified to replace the carbon source with prebiotics, allowing for the analysis of bacterial metabolism (Corcoran *et al.*, 2005).

From an experimental point of view, in vitro fermentation assays constitute an essential step in understanding the selectivity and fermentability of XOS-rich extracts, simulating the physiological conditions of the large intestine (Álvarez *et*

al., 2023; Rycroft *et al.*, 2001). These models allow for the evaluation of bacterial growth, SCFA production, pH variation, and substrate consumption, using human fecal inoculum to realistically represent the gut microbiota. In this context, the present study aimed to evaluate the prebiotic and antioxidant effect of the XOS-rich extract obtained from a *Eucalyptus* byproduct. To this end, assays were conducted using the strains Lactobacillus acidophilus and Lacticaseibacillus rhamnosus, as well as the in-batch colonic fermentation system.

2. MATERIAL AND METHODS

2.1. Obtaining a *Eucalyptus*-based prebiotic

The XOS-extract (prebiotic) was obtained from a hemicellulosic hydrolysate (HH) derived from a *Eucalyptus* byproduct, consisting of sawdust generated during log cutting in the pulp industry, from a mixture (1:1, w/w) of *Eucalyptus grandis* and *Eucalyptus urophylla* species. The hydrothermal pretreatment (HP) was carried out in a chemical reactor (Regmed™) equipped with stainless steel digesters (1.5 L), with mechanical agitation and temperature and pressure control. In each digester 50 g (dry weight) of the byproduct and 500 mL of distilled water (10%, w/v) were added. The mixture was heated to 160 °C in approximately 40 min, remaining at this temperature for 65 min. After natural cooling at 25 °C (~6 h), the HH was filtered through a sintered glass filter (porosity number 3) and stored at -20 °C until use, as described by Otaviano et al. 2023.

2.2. Purification of the *Eucalyptus*-based prebiotic

The purification step was conducted according to the protocols described in the same reference. Otaviano et al. 2023, with the aim of removing interfering compounds and concentrating on the oligosaccharides of interest. Initially, the HH was concentrated by vacuum evaporation in a stainless steel rotary evaporator (Heidolph), operating at 50 °C, 200 mbar for 10 min, followed by 100 mbar for 50 min. Then, liquid-liquid extraction (LLE) was performed using ethyl acetate (EtOAc) in a 1:1 (v/v) volumetric ratio. The aqueous and organic phases were mixed in 50 mL Falcon™ tubes and orbitally shaken at 300 rpm for 5 min at 25 °C. After shaking, the samples were left to stand in a separatory funnel for 30 min to ensure complete phase separation. The resulting phases were carefully

separated, their volumes were measured, and they were stored at -20 °C until later use. This process resulted in obtaining a purified extract rich in XOS, which was used in the subsequent steps of this study.

2.3. Evaluation of prebiotic activity in vitro

2.3.1. Evaluation of prebiotic activity

The probiotic strains *Lacticaseibacillus rhamnosus* and *Lactobacillus acidophilus* were activated and cultured in MRS broth (Man, Rogosa and Sharpe) supplemented with glucose at 36.5 °C, under anaerobic conditions for 24 h. The number of cells used in each assay was determined at the time of inoculation by counting colony-forming units (CFU.mL^{-1}) on MRS agar, adjusting the inoculum to 1 × 10^{6} CFU.mL^{-1}. To determine the basal growth conditions of the strains, growth curves were obtained in MRS broth with and without glucose, to characterize the microbial behavior in the absence of prebiotic sources.

The in vitro prebiotic activity assay was conducted according to the method described by Meral et al. 2024, with adaptations. The strains were inoculated (1 × 10^{6} CFU.mL^{-1}) in glucose-free MRS broth supplemented with 1% (w/v) of the XOS-rich extract. Chicory inulin 1% (w/v) was used as a positive control, while MRS medium without added carbohydrate was adopted as a negative control.

Bacterial growth was monitored by optical density (OD_{600}) using a Genesys 50 UV-Vis spectrophotometer (Thermo Scientific, Waltham, MA, USA) at 0, 2, 4, 6, 8, 12, 24, and 48 h incubation intervals under anaerobic conditions. Statistical analysis was performed using GraphPad Prism 9.0 software (GraphPad Software, San Diego, CA, USA). The results were expressed as mean ± standard error of the mean (SEM) of three independent experiments. Differences between groups were assessed by two-way ANOVA, considering significance levels of *p ≤ 0.05; **p ≤ 0.01; ***p ≤ 0.001.

2.3.2. Determination of short-chain fatty acids (SCFAs) production

The quantification of short-chain and branched-chain fatty acids was performed by gas chromatography (GC), after extraction of the compounds according to a modified protocol from Zhao et al. 2006. For each sample, 200 mg were weighed into 2 mL microtubes, to which 200 µL of ultrapure water were

added. A metal sphere was then inserted, and the contents were stirred for 15 min until completely homogeneous. The pH of the mixture was adjusted to 2–3 by adding 0.6 M hydrochloric acid, followed by further stirring for 10 min at 25 °C. Subsequently, the samples were centrifuged at 14,000 rpm for 10 min, also at 25 °C, promoting the separation of the aqueous and organic phases. For GC analysis, 96 µL of the organic phase were collected and added to 4 µL of internal standard solution (1000 ppm biphenyl), this mixture being transferred to vials with inserts, which were then inserted into the GC carousel.

The analysis was conducted on an Agilent 7890B gas chromatograph equipped with a flame ionization detector (FID) and an Agilent 125-7032 capillary column (30 m × 0.53 mm × 1.0 µm). Helium was used as the carrier gas, with a flow rate of 3.4 $mL.min^{-1}$ and a pressure of 3 psi. The injection volume was 1 µL in splitless mode (15 $mL.min^{-1}$ for 0.75 min). The temperature program started at 80°C for 0 min, increasing by 10°C.min^{-1} until reaching 230°C, remaining at this value for 2 min. The injector and detector temperatures were maintained at 250 °C. Auxiliary gas flows: hydrogen at 30 $mL.min^{-1}$, air at 300 $mL.min^{-1}$, and nitrogen (makeup) at 25 $mL.min^{-1}$. The data were acquired and processed using the OpenLab CDS ChemStation software. The identification of the SCFAs was performed by comparing the retention times with those of a mixture of analytical standards. The quantification was based on previously established analytical curves. The results were expressed according to the official AOAC 996.06 method.

2.3.3. Evaluation of the cytotoxicity of the XOS-extract

Cytotoxicity was evaluated using resazurin hydrochloride (Sigma-Aldrich), a redox indicator that allows monitoring of cell viability through fluorescent and colorimetric changes, according to Page et al. (1993).

Human colorectal adenocarcinoma cells Caco-2 (BCRJ nº 0059) were cultured in monolayer in 75 cm^2 flasks (Corning) at 37°C, 5% CO_2 and 95% air, under saturated humidity, in Dulbecco′s Modified Eagle′s Medium (DMEM) supplemented with 10% Fetal Bovine Serum (Gibco). For the assay, cells were seeded in 96-well microplates at 1 × 10^4 cells/well and incubated for 24 h for adhesion.

The extract was dissolved in 10% dimethyl sulfoxide (DMSO) and diluted in the culture medium, testing serial concentrations from 31.2 to 1000 μg.mL^{-1}. Controls included negative (no treatment), solvent (0.1% DMSO), and positive (50% DMSO). After 24 h of treatment, the medium was replaced with 50 μL of 0.01% (w/v) resazurin, and the plates were incubated for 4 h. Fluorescence was measured using a CaryEclipse spectrofluorometer (Agilent Technologies) with excitation/emission at 560/590 nm.

Results were expressed as a percentage of viability relative to the negative control (100%) and presented as mean ± standard deviation of triplicates in three independent experiments. Normality was verified by the Kolmogorov-Smirnov test, followed by ANOVA and Dunnett's post-hoc test. The IC_{50}, corresponding to the concentration that reduces cell viability by 50%, was calculated using GraphPad Prism 7.0 (San Diego, CA, USA).

2.3.4. In vitro batch fermentation

In vitro batch fermentation (Guimarães et al., 2023) was employed to investigate the acute effect of administering different doses of an XOS-rich extract (prebiotic) on the human gut microbiota. Fermentations were conducted in independent reactors (70 mL) for 48 h, using fecal inoculum from healthy individuals. Three healthy individuals (two women and one man) were selected for the study. Fecal samples were collected and processed according to a methodology previously described by Bianchi et al. 2018. Briefly, the fecal suspension used in the experiment was prepared in anaerobic phosphate buffer containing Na_2HPO_4, NaH_2PO_4, and sodium thioglycolate, prepared individually for each participant and stored at -20 °C until use.

Doses corresponding to 8.7 mg, 17.4 mg, and 24.5 mg of XOS extract were evaluated in triplicate to simulate different intake levels of XOS extract. Control assays were conducted under the same conditions, replacing the ingredient with distilled water. Comparison between the results obtained in the controls and in the treated samples allowed us to determine the specific effect of the prebiotic on the microbiota.

For fermentation, a low-sugar basal nutrient medium buffered at pH 6.5 was used, containing nutrients representative of the colonic environment (3.5 g.L^{-1} K_2HPO_4, 10.9 g.L^{-1} KH_2PO_4, 2.0 g.L^{-1} $NaHCO_3$, 2.0 g.L^{-1} yeast extract, 2.0 g.L^{-}

^{1} peptone, 0.5 g.L^{-1} cysteine, 2.0 g.L^{-1} Tween 80, 2.0 g.L^{-1} glucose, 2.0 g.L^{-1} starch and 1.2 g.L^{-1} resazurin (0.1%, w/v). The medium was co-administered with the ingredient at the beginning of fermentation.

All experiments were performed in triplicate, corresponding to four independent colonic fermentations conducted in parallel for each experimental condition.

2.3.5. Prebiotic Index (PI)

Ensure the reproducibility of the in vitro prebiotic activity assay and to allow for proper interpretation of the results, the culture media used, as well as the experimental incubation conditions (time, temperature, and atmosphere), were organized and summarized in Table 1.

Table 1. Culture media and incubation conditions for the in vitro prebiotic activity assay.

Microbial groups	Culture medium	Incubation	Conditions
Bifidobacterium spp.	BIM-25 agar	37 °C / 72 h	Anaerobic
Lactobacillus spp.	MRS agar	37 °C / 72 h	Anaerobic
Clostridium spp.	Reinforced Clostridial Agar	37 °C / 72 h	Anaerobic
Total anaerobes	Standard Methods Agar	37 °C / 72 h	Anaerobic

The total bacterial load and selected genera were enumerated at the beginning of the study (end of the control period) and at the end of colonic fermentation by plate count. To quantify the prebiotic effect, duplicate samples were collected from the colonic fermentation vessels with and without treatment at different times. The Prebiotic Index (PI) is calculated according to Equation 1:

$$PI = (Bif/Total) - (Bac/Total) + (Lac/Total) - (Clos/Total) \quad (1)$$

Where:

Bif = number of Bifidobacterium spp. after fermentation minus the number at the beginning of the study.

Bac = number of Bacteroides spp. after fermentation minus the numbers at baseline.

Lac = number of Lactobacillus after fermentation minus the numbers at baseline.
Clos = number of Clostridium perfringens after fermentation minus the numbers at baseline.

Total = total number of bacteria after fermentation minus the baseline numbers.

The IP equation assumes that an increase in bifidobacteria and/or lactobacilli populations is positive, while an increase in bacteroides and clostridia (histolyticum subgroup) is negative. The IP equation offers the advantage of normalizing changes in the bacterial population relative to initial microbial levels, considering the physiological variability that characterizes the experimental process of in vitro fermentation (De Oliveira *et al.*, 2025).

2.3.6. Quantification of SCFAs in colonic ferments

The quantification of SCFAs (acetic, propionic, and butyric acids) followed the method described by Dostal et al. 2014. Briefly, 2 mL of colonic fermentation samples were centrifuged at 14,000 rpm for 5 min, and 1 mL of the supernatant was diluted 1:1 in ultrapure water. The solution was filtered through 0.45 µm Millex^{TR} filters before injection into an Agilent HP-6890 GC (Agilent Technologies, Santa Clara, CA, USA), coupled to an Agilent HP-5975 mass selective detector and equipped with a DB-WAX capillary column (60 m × 0.25 mm × 0.25 µm).

The analysis conditions were: injection at 220 °C; column temperature starting at 35 °C, with ramps of 2 °C.min^{-1} to 38 °C, 10 °C.min^{-1} to 75 °C, 35 °C.min^{-1} to 120 °C (1 min), 10 °C.min^{-1} to 170 °C (2 min), and 40 °C.min^{-1} to 250 °C (2 min); detector at 250 °C. Helium was used as carrier gas at 1 mL.min^{-1}. Analytical curves were constructed using stock solutions of analytical standards of acetic, propionic, and butyric acids. Samples were analyzed in triplicate for each replicate of the ascending colon, before and after treatment. Results were expressed in mmol.L^{-1}.

2.3.7. Quantification of ammonia ions

Ammonia concentrations were evaluated in triplicate for each fermentation reactor using a dedicated ionometer (model HI 4101, Hanna Instruments, USA)

in conjunction with an ammonium ion selective electrode (model Orion 95-12, Thermo Fisher Scientific, USA). A 0.2 mL aliquot of an ammonia ionic strength adjustment solution (Orion) was added to 10 mL of each sample (Bianchi *et al.*, 2018).

2.3.8. Analysis of microbiota composition using 16S rRNA sequencing

Microbiota analysis was conducted by sequencing the hypervariable regions of the 16S and ITS rRNA genes using the Illumina platform with paired reading (PE250). Samples were prepared with specific primers containing adapters compatible with the technology.

The raw sequencing files (FASTQ) were processed in the quantitative insights into microbial ecology (QIIME2) environment, following a standardized pipeline for amplicon analysis. For both markers, primers were removed with Cutadapt, and sequences underwent quality filtering, chimera removal, and Amplicon sequence variants (ASVs) inference with the DADA2 algorithm. Taxonomic classification was performed using the SILVA database for 16S and the UNITE database, in conjunction with DADA2, for ITS (Bymycell Inova Simples Ltda., 2025).

Alpha and beta diversity analyses, visualizations with interactive graphs, rarefaction analyses, and statistical analyses were performed for both markers.

2.4. Evaluation of the antioxidant activity of XOS-extract

2.4.1. 2,2-Diphenyl-1-picrylhydrazyl (DPPH) free radical scavenging assay

The antioxidant activity was evaluated by the DPPH free radical scavenging assay. In a microplate, 20 µL of the extract were added to 200 µL of 0.06 mM DPPH solution (Sigma). After 20 min of incubation, the absorbance was measured at 517 nm in a microplate reader. Ultrapure water was used as a solvent for the preparation containing XOS and inulin, and solutions were prepared with the following concentrations: 5, 10, 25, 50, 100, 150, 250, 500, 1000, 2000, 3000, 4000, 6000, and 8000 $\mu g.mL^{-1}$. Additionally, a 2 mL solution of ethanol containing 0.1 mM DPPH was prepared, to which 2 mL of the

previously dissolved samples were added. After 20 min of incubation at 25 °C, 200 µL of the solution were transferred to a blank 96-well microplate, and the absorbance was measured at 517 nm using a multimode microplate reader.

DPPH radical scavenging was calculated using Equation 2:

DPPH consumption (%) = ((Ac - As) / Ac) × 100% (2)

Where:
Ac = absorbance of the control.
As = absorbance of the sample.

The antioxidant activity of the samples was expressed as EC_{50}, being the antioxidant concentration that provided a 50% reduction of DPPH radicals. Trolox (0-8000 µg.mL^{-1}, dissolved in ethanol), a reference antioxidant, was used to compare the antioxidant capacities of the samples (Zhang, Liangqing *et al.*, 2019) see Supplementary Material, Section 6.

2.4.2. Ferric reducing antioxidant power (FRAP)

In a dark environment, 20 µL of the extract were pipetted into a microplate, followed by the addition of 30 µL of distilled water and 200 µL of the FRAP solution. The FRAP reagent was prepared immediately before use, consisting of a mixture of 0.3 M acetate buffer (pH 3.6), 10 mM 2,4,6-tris(2-piridil)-s-triazina) (TPTZ) dissolved in 40 mM hydrochloric acid, and 20 mM aqueous ferric (III) chloride hexahydrate, in a 10:1:1 ratio. After the reagent was added, the mixture was homogenized and incubated at 37 °C for 8 min. The absorbance was then measured at 595 nm using a microplate reader. The quantification of antioxidant potential was performed based on a ferrous sulfate standard curve, ranging from 100 to 800 µM, and the results were expressed in mM of ferrous sulfate. For the specific evaluation of the XOS-extract, 200 µL of FRAP solution were mixed with 30 µL of XOS-extract solution (3000 µg.mL^{-1}) and 20 µL of distilled water in a blank 96-well microplate. The mixture was stirred for 1 minute and incubated at 37 °C for 30 min before absorbance reading at 593 nm using a microplate reader. Trolox (0-8000 µg.mL-1, dissolved in ethanol), a reference antioxidant, was used

to compare the antioxidant capacities of the samples (Zhang, Liangqing *et al.*, 2019).

Equation 3 was used to calculate antioxidant activity using the FRAP method:

FRAP Activity (%) = (Ab / As − Ab) × 100 (3)

A_s = absorbance of the sample

A_b = absorbance of the blank

The EC_{50} value (effective antioxidant concentration to consume 50% of the substrate) was obtained from the non-linear fitting of experimental data on concentration and percentage of antioxidant activity, using the least squares method (Levenberg–Marquardt) in OriginPro software (OriginLab Corp., USA).

The DPPH and FRAP assays were fitted to an arctangent mathematical model. From the parameters obtained, the concentration corresponding to 50% of the response was calculated, expressed as EC_{50} (see Supplementary Material Section 6).

2.4.3. Statistical analyses

Data were expressed as mean ± standard deviation (SD). Statistical significance was assessed using paired t-tests, one-way analysis of variance (ANOVA), and Tukey's test, with a significance threshold of $p < 0.05$. Analyses were performed using GraphPad Prism software, version 8.0 (La Jolla, CA, USA). The uncertainty associated with EC_{50} was determined by error propagation, considering the uncertainties of the adjusted parameters and assuming independence between them (see Supplementary Material Section 6). The results were expressed as EC_{50} ± uncertainty, corresponding to the mean and standard deviation of the concentration required to achieve 50% substrate consumption. Lower EC_{50} values indicate a higher antioxidant capacity of the evaluated extract.

3. RESULTS

3.1. In vitro cultures of probiotic bacteria with XOS-extract supplementation

Figures 1 and 2 illustrate the growth profile of *Lactobacillus acidophilus* and *Lacticaseibacillus rhamnosus* when supplemented with XOS-extract and inulin, as well as the behavior observed in the negative control, over 48 h of incubation.

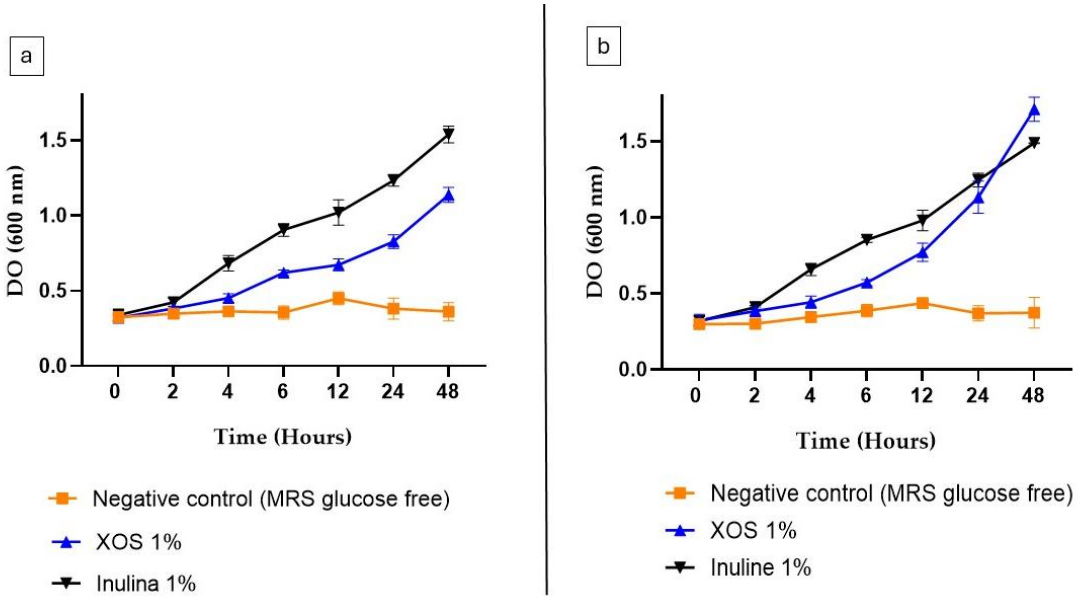

Figure 1. Prebiotic effect of XOS on the growth of *Lacticaseibacillus rhamnosus* (a) and *Lactobacillus acidophilus* (b) in glucose-free MRS medium. Inulin was used as a positive control and carbohydrate-free MRS as a negative control.

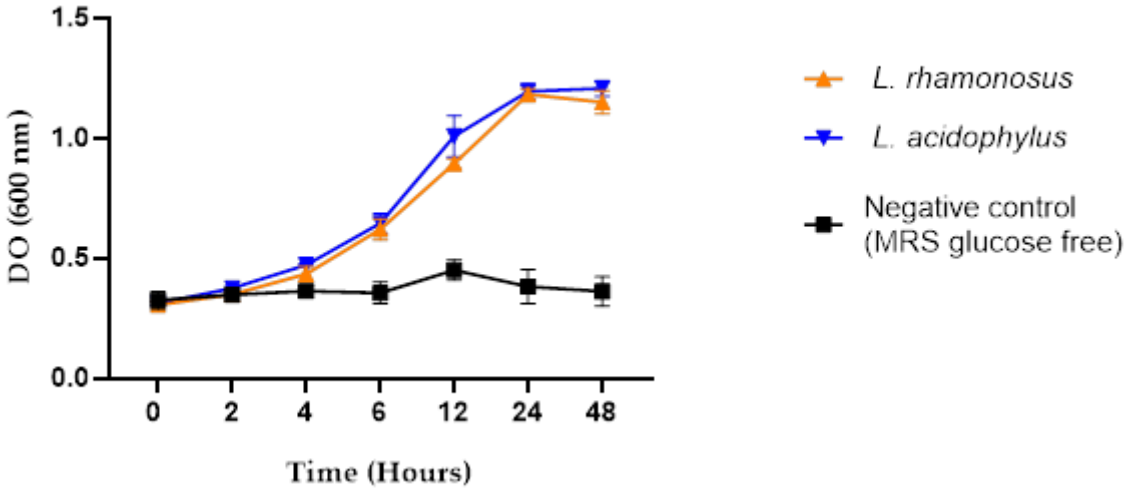

Figure 2. Growth curve of *Lactobacillus acidophilus* and *Lacticaseibacillus rhamnosus* in MRS medium with glucose after 48 h of incubation and MRS without glucose as a negative control. No statistically significant differences were found between them (ANOVA/Tukey, $p > 0.05$).

The results obtained in the prebiotic activity assay (Figure 1) showed a significant increase in the growth of *Lactobacillus acidophilus* and *Lacticaseibacillus rhamnosus* when cultivated in the presence of XOS-extract from 6 h of incubation, reaching the maximum growth level at 48 h. However, it was observed that *Lactobacillus acidophilus* showed a greater population increase after 24 h of incubation compared to *Lacticaseibacillus rhamnosus*. Similarly, inulin supplementation in the cultures resulted in a higher growth rate for *Lactobacillus rhamnosus* compared to that observed with XOS-extract, indicating a greater prebiotic effect of inulin for this strain. Therefore, XOS-extract shows potential for prebiotic activity, favoring the growth of probiotic bacteria, although to a lesser extent when compared to inulin. On the other hand, no significant differences were observed in the growth of probiotic strains in the negative control group after 48 h of incubation.

The growth of *Lactobacillus acidophilus* and *Lactobacillus rhamnosus* in MRS medium supplemented with glucose (Figure 2) showed typical profiles of lactic acid bacteria, with a short lag phase, followed by a rapid increase in OD_{600} until the stationary phase. Both strains exhibited similar kinetic behavior over time, indicating good adaptation to the medium and efficient use of glucose as a carbon source.

3.2. Fatty acid production profile of Lactobacillus cultures with XOS-extract supplementation

In the present study, the levels of these compounds were quantified after 48 h of growth of *Lactobacillus acidophilus* and *Lacticaseibacillus rhamnosus*, allowing us to evaluate differences in the metabolic profile between the strains (Tables 2 and 3, respectively).

Table 2. Short-chain fatty acids (SCFAs) content in *Lactobacillus acidophilus* and *Lacticaseibacillus rhamnosus* cultures supplemented with XOS after 48 h of growth.

Fatty acid	*L. acidophilus* 48 h (μg·mL⁻¹)	*L. rhamnosus* 48 h (μg·mL⁻¹)
Acetic acid	0.00661	0.00698
Propionic acid	0.02383	0.02550
Butyric acid	0.57482	1.51428
Total SCFA	0.60526	1.54676

Source: Experimental data (n = 1).

Table 3. Medium-chain fatty acids (MCFAs) content after 48 h of culture of *Lactobacillus acidophilus* and *Lacticaseibacillus rhamnosus*.

Fatty acid	*L. acidophilus* 48 h (μg·mL⁻¹)	*L. rhamnosus* 48 h (μg·mL⁻¹)
Isobutyric acid	1.48815	1.71723
Isovaleric acid	0.01252	0.01339
Valeric acid	0.19441	0.21050
Total MCFA	1.69508	1.94112

Source: Experimental data (n = 1).

3.3. Determination of the cytotoxicity of the XOS-rich extract

The culture supplemented with XOS showed a dose-dependent effect on the viability of Caco-2 cells. Lower doses (31.2, 62.5, and 125 μg.mL^{-1}) did not differ significantly from the negative control, indicating the absence of a relevant cytotoxic effect at these levels. However, at doses from 250 μg.mL^{-1} onwards, a gradual reduction in cell viability was observed. These results indicate that the XOS-extract exerts a cytotoxic effect at higher doses, while maintaining biocompatibility at lower doses (Figure 3).

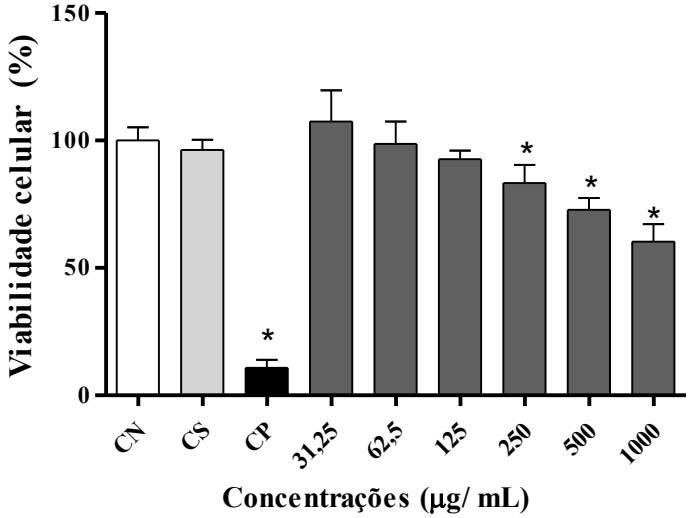

Figure 3. Viability of Caco-2 cells treated for 24 h with different doses of the XOS-extract.
**Significantly different from the negative control (ANOVA, Dunnett, p < 0.05). Values are presented as mean and standard deviation of the calculated percentage of cell viability.*
CN: negative control; CS: solvent control; CP: positive control.

3.4. SCFAs production in vitro colonic simulation assays

Figure 4 presents the results of the quantification of SCFAs obtained after 48 h of in vitro fermentation, simulating the conditions of the human colon.

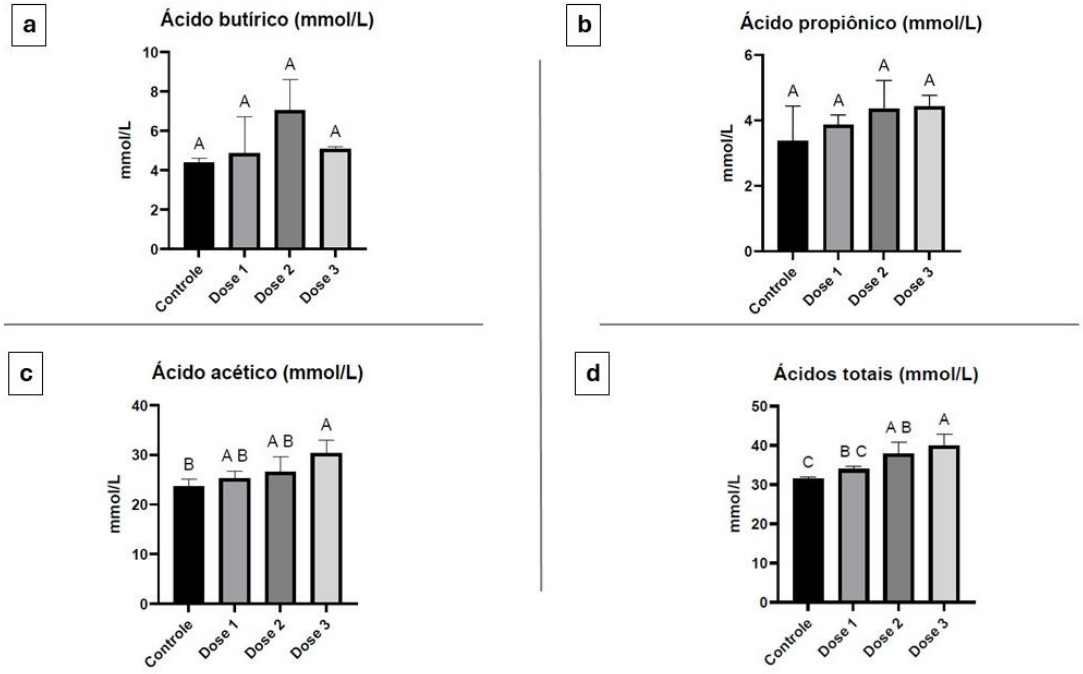

Figure 4. Production of short-chain fatty acids (SCFAs) in 48 h in a short-term in vitro simulation of the colon, with microbiota from healthy adults. Three doses of

XOS-extract were administered, besides of control assay (without XOS-extract addition).
The assays were performed in triplicate.
Different letters indicate a statistically significant difference ($p<0.01$) in the same column, according to Tukey's post-hoc test.
Doses: 1=8.7 mg. 2=17.4 mg. 3=24.5 mg.

3.5. Prebiotic index (PI) in vitro colonic simulation assays

The PI index assesses the ability of a substrate to selectively modulate the intestinal microbiota, stimulating beneficial genera and reducing potentially pathogenic ones (Pessotti et al., 2025). Table 4 presents the effect of different doses of the XOS-extract on microbial abundance and PI after 48 h of in vitro fermentation in the microbiota of healthy adults.

Table 4. Effect on the abundance of selected genera and prebiotic index (PI) of each treatment after 48 h of short-term in vitro simulation.

Treatment	Total anaerobes	*Bifidobacterium spp.*	*Lactobacillus spp.*	*Clostridium spp.*	*Bacteroides spp.*	*Prebiotic Index*
Control	8.48 ± 0.32[a]*	5.92 ± 0.12[b]	6.80 ± 0.31[a]	8.64 ± 0.41[a]	9.30 ± 0.02[a]	−0.57 ± 0.04[c]
Dose 1	8.22 ± 0.10[a]	6.48 ± 0.22[a]	6.95 ± 0.13[a]	8.30 ± 0.13[a]	7.31 ± 0.02[b]	−0.30 ± 0.04[b]
Dose 2	8.22 ± 0.10[a]	6.67 ± 0.11[a]	6.94 ± 0.05[a]	8.37 ± 0.09[a]	7.34 ± 0.05[b]	−0.26 ± 0.04[a]
Dose 3	8.37 ± 0.10[a]	5.92 ± 0.35[b]	6.67 ± 0.04[a]	8.22 ± 0.07[a]	7.29 ± 0.01[b]	−0.33 ± 0.07[b]

Microbial quantification was performed by plate count and expressed in log CFU.mL-1.
**Different letters indicate a statistically significant difference (P<0.05) in the same column, according to Tukey's post-hoc test.*
Doses: 1=8.7 mg. 2=17.4 mg. 3=24.5 mg.

3.6. Determination of ammonia content in in vitro colonic simulation assays

During colonic fermentation, the NH_4^+ content reflects the degree of proteolytic activity (degradation of proteins and amino acids) of the microbiota. Reductions in NH_4^+ indicate the predominance of a sacrolytic fermentation (based on the use of carbohydrates and prebiotic fibers), characteristic of a more beneficial intestinal environment (Diether; Willing, 2019).

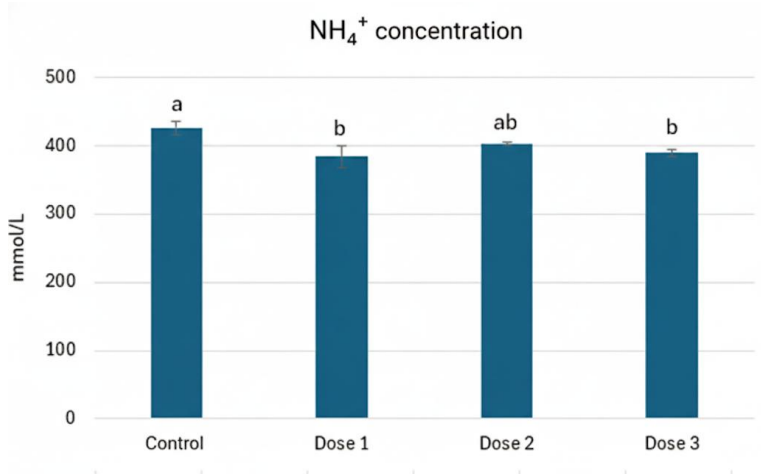

Figure 5. NH_4^+ levels (mmol.L^{-1}) after 48 h of short-term in vitro colonic simulation.
Groups followed by different letters differ significantly from each other by Tukey's test ($p<0.05$). Doses: 1=8.7 mg. 2=17.4 mg. 3=24.5 mg.

3.7. Determination of microbiota composition in vitro colonic simulation assays

The results presented from this topic should be considered preliminary observations, since the complete bioinformatic treatment will still be conducted by a professional, with the aim of ensuring greater accuracy in taxonomic inferences.

The taxonomic characterization of the microbiota is an essential step in understanding the structure, diversity, and possible ecological functions of the microbial communities present in the analyzed samples. Assessment at different hierarchical levels, such as phylum, order, family, and genus, allows us to observe the relative distribution of microorganisms and identify predominant groups that may be associated with specific physiological conditions or responses to experimental treatments.

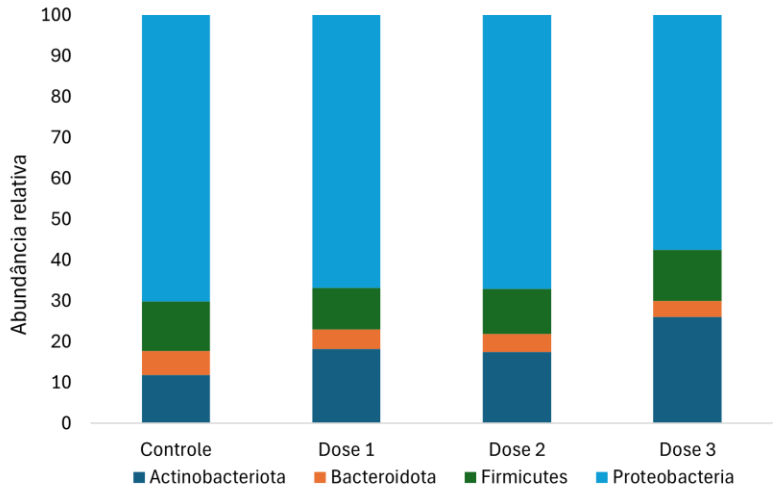

Figure 6. Relative abundance of microbiota phyla in vitro colonic simulation assays.
Doses: 1=8.7 mg. 2=17.4 mg. 3=24.5 mg.

Figure 7 shows the relative abundance profile of the predominant bacterial order, highlighting the variations observed between the control group and the assays supplemented with XOS-extract.

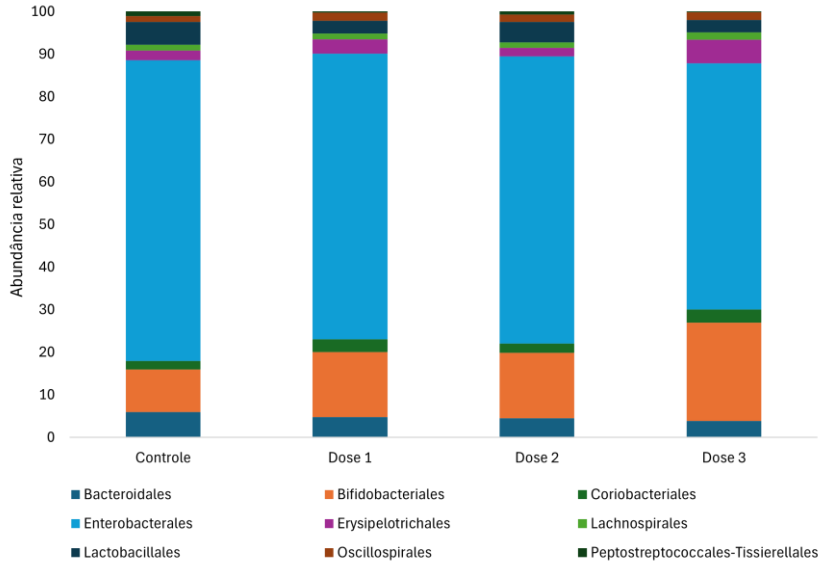

Figure 7. Relative abundance of microbiota order in vitro colonic simulation assays.
Doses: 1=8.7 mg. 2=17.4 mg. 3=24.5 mg.

Figure 8 shows the modulation of microbiota at the family level, highlighting the differences observed between the control assay and those supplemented with XOS-extract at different doses.

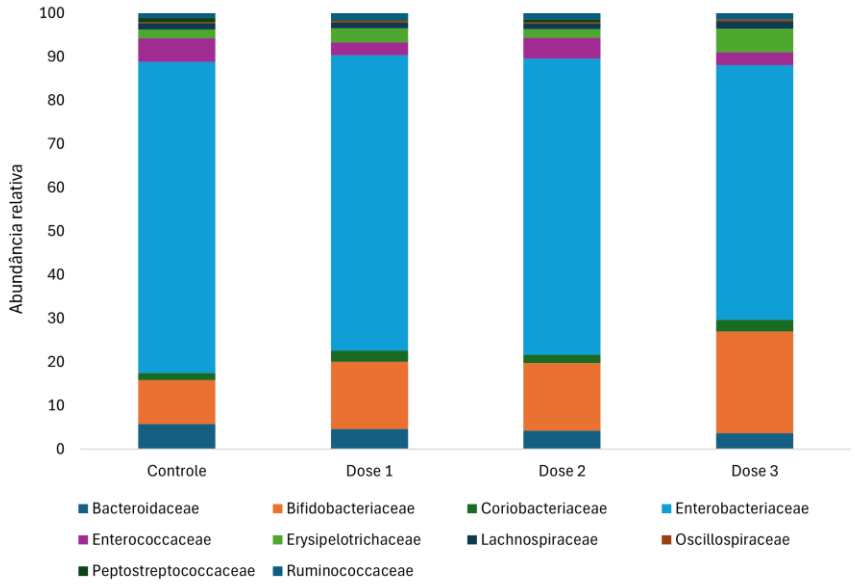

Figure 8. Relative abundance of microbiota family in vitro colonic simulation assays.
Doses: 1=8.7 mg. 2=17.4 mg. 3=24.5 mg.

The relative distribution of the main bacterial genera, observed in Figure 9, highlights the differences between the control assay and those supplemented with XOS at different doses.

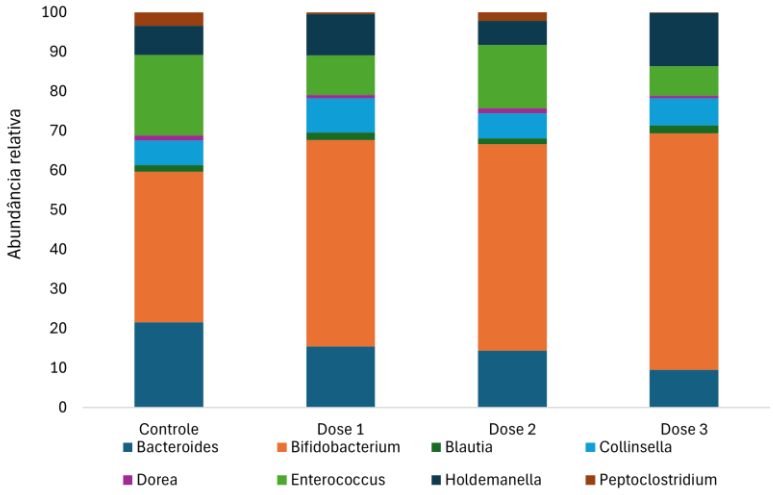

Figure 9. Relative abundance of microbiota genus in vitro colonic simulation assays
Doses: 1=8.7 mg. 2=17.4 mg. 3=24.5 mg.

3.8. Microbiota diversity index in vitro colonic simulation assays

Microbial diversity was evaluated using the Chao1 and Shannon indices, which represent, respectively, species richness and total diversity considering the richness and uniformity of the bacterial community. Figure 10 shows the

comparison of these parameters between the control assay and those supplemented with XOS-extract, allowing the evaluation of possible variations in the structure of the intestinal microbiota after in vitro fermentation.

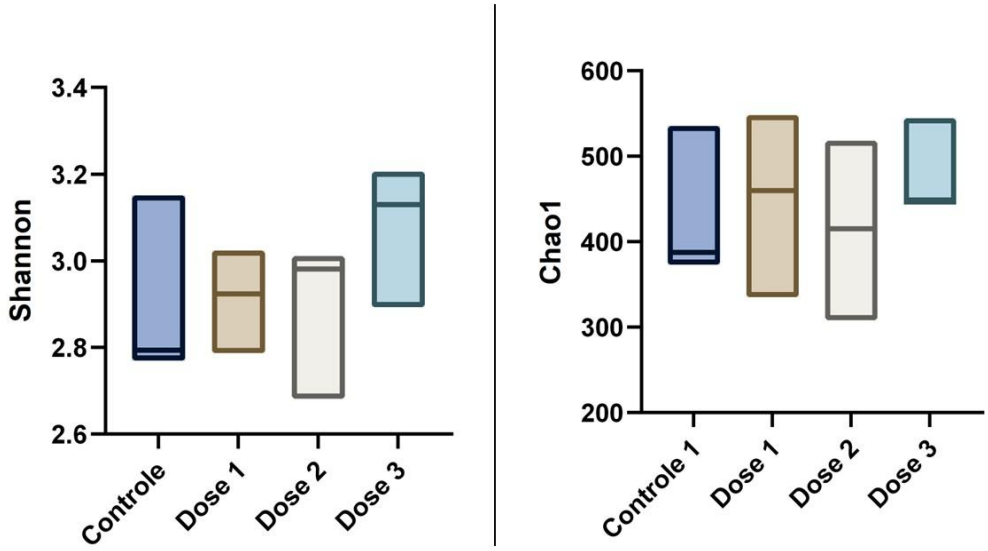

Figure 10. Boxplot analysis of Shannon and Chao1 alpha-diversity indices obtained from short-term in vitro dynamic colonic simulation.
Doses 1=8.7 mg. 2=17.4 mg. 3=24.5 mg.

The results compare the gut microbiota of healthy adults prior to XOS-extract supplementation (control) and after administration of doses 1, 2, and 3 of XOS-extract. No statistically significant differences were observed in the alpha-diversity indices after XOS-extract supplementation.

The Chao1 and Shannon indices did not show statistically significant differences ($p>0.05$) between the control assay and the XOS-extract supplemented assay, indicating that supplementation did not significantly alter microbial diversity under the assays conditions. This stability suggests that the short fermentation time was insufficient to promote marked structural changes in the bacterial community.

The antioxidant activity of the XOS-extract was evaluated using the following methods: FRAP and DPPH, using Trolox (a strong reference antioxidant) and inulin (a prebiotic commonly used in the literature) as comparison standards, as illustrated in Figure 11ab, respectively.

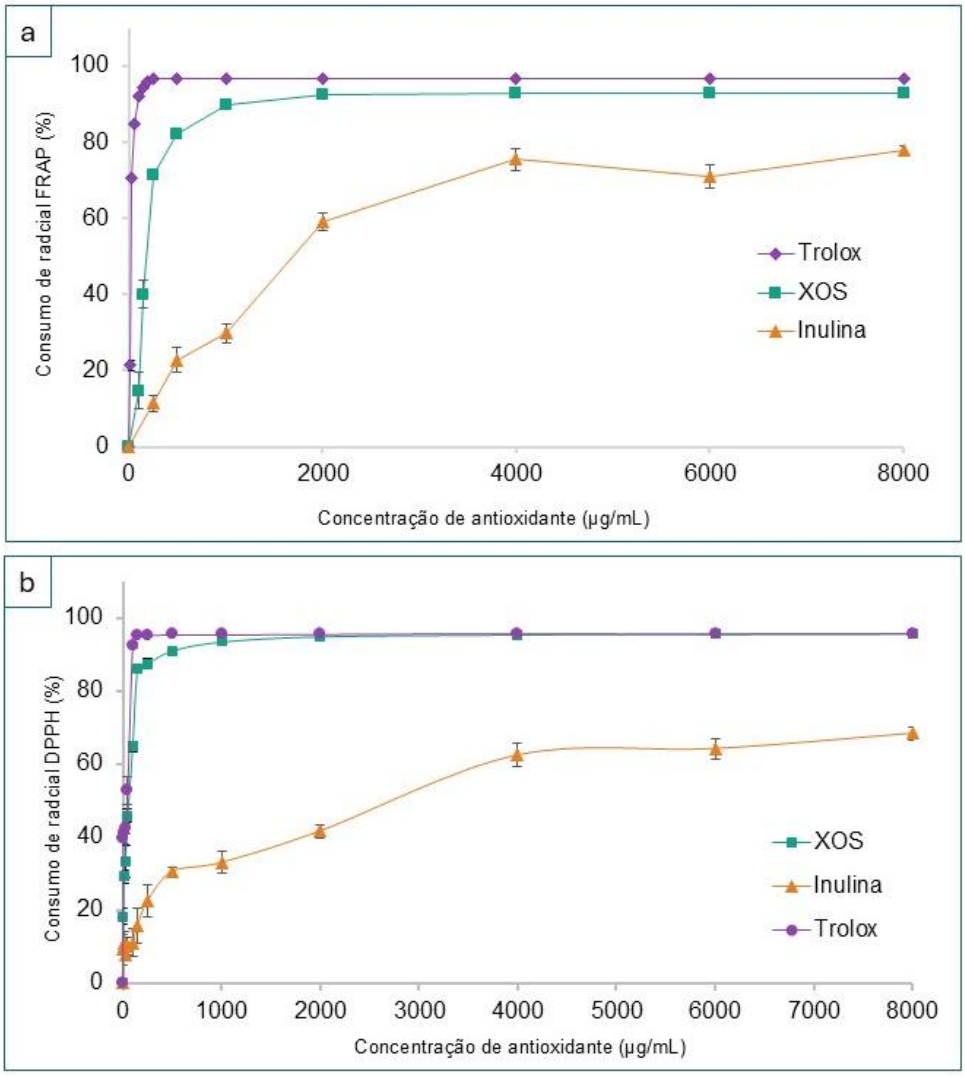

Figure 11. Antioxidant activity of Trolox, XOS-extract, and inulin evaluated by the following methods: (a) FRAP, (b) DPPH at different concentrations (0-8000 $\mu g.mL^{-1}$). Results are expressed as percentage of radical scavenging (%). Data are presented as mean ± standard deviation (n=4).

The FRAP method (Figure 11a) showed similar results to the DPPH method (Figure 11a), resulting in a significant reduction capacity of ferric ion (Fe^{3+}) to ferrous ion (Fe^{2+}), with a response dependent on the concentration of XOS-extract, Trolox, and inulin. However, the DPPH method showed a slightly higher antioxidant activity rate for XOS and Trolox when compared to the FRAP method. Conversely, the FRAP method showed a slightly higher rate for inulin when compared to the DPPH method.

In the DPPH method (Figure 11b), was demonstrated increased of antioxidant activity as a function of XOS-extract concentration, reaching a maximum radical consumption level of approximately 96% when the XOS-extract

content 1000 μg.mL^{-1}. This result was similar to Trolox, which also quickly reached a maximum radical consumption level of approximately 96%, however, with a Trolox content of less than 1000 μg.mL^{-1}. Therefore, although Trolox demonstrated greater antioxidant potential, being an antioxidant standard, the XOS exhibited expressive performance. In the case of inulin, an increase in antioxidant activity was also observed as a function of its content, reaching a maximum radical consumption of approximately 68%, which corresponded to an inulin content of 8000 μg.mL^{-1}, however, in this case the level was not reached, presenting a smoother slope (rate) of the curve when compared to XOS and Trolox.

In order to establish a quantitative value for comparison with the literature, the EC_{50} values of the curves of the respective assays were calculated. EC_{50} expresses the concentration of antioxidant needed to consume 50% of the radical for each method evaluated (Table 5).

Table 5. EC_{50} values of the FRAP and DPPH antioxidant assays for XOS-extract, inulin, and Trolox.

Sample	EC_{50} FRAP	EC_{50} DPPH
XOS	188.76 ± 10.32	44.10 ± 2.34
Inulin	1631.88 ± 79.50	1634.24 ± 310.67
Trolox	16.54 ± 0.78	21.05 ± 2.89

The EC_{50} values demonstrate differences in the antioxidant capacity of XOS-extract among the different methods employed. The lowest EC_{50} value for the DPPH method indicates that this system was the most sensitive to the antioxidant action of the XOS-extract, while the FRAP method showed a higher concentration demand for XOS to achieve the same 50% substrate consumption. However, these variations are expected, as each assay responds differently to the antioxidant capacity of the samples studied. Furthermore, when compared to reference standards, such as Trolox, which has a high antioxidant capacity as it is a vitamin E analog, and inulin, a widely used prebiotic generally with lower direct antioxidant activity, XOS-extract demonstrate an intermediate activity profile, reinforcing their potential as a multifunctional functional ingredient.

4. DISCUSSION

XOS are recognized as prebiotics capable of selectively stimulating the growth of beneficial microorganisms in the gastrointestinal tract, especially bacteria of the genera Lactobacillus and Bifidobacterium. The evaluation of in vitro prebiotic activity allows us to understand the potential of these compounds to promote the multiplication of probiotic strains and to compare them to other commercial products with prebiotic action, such as inulin (Nogueira-Prieto, Natalia-María *et al.*, 2025). The results obtained demonstrate that the XOS-extract derived from *Eucalyptus* byproduct presents relevant functional properties, with prebiotic effects in isolated cultures, partial metabolic modulation in short-duration colonic fermentations, and significant antioxidant activity. In general, the findings are aligned with the body of evidence previously described for XOS-extract obtained from lignocellulosic biomass (Aachary; Prapulla, 2011; Míguez *et al.*, 2021; Samanta *et al.*, 2015).

The results showed that *Lacticaseibacillus rhamnosus* and *Lactobacillus acidophilus* exhibited superior growth when cultured with XOS and inulin, compared to the negative control (MRS without glucose), confirming the ability of these non-digestible carbohydrates to act as fermentable substrates for probiotic genera. This behavior is consistent with studies by Aachary et al. 2011 XOS who evaluated xylooligosaccharides obtained from lignocellulosic xylan by controlled hydrolysis and demonstrated a high selectivity of XOS toward *Lactobacillus* and *Bifidobacterium*, promoting increased cell density and reduced lag phase due to their low degree of polymerization and rapid assimilation. Although the XOS evaluated in that study were produced from xylan-rich biomass and not from hydrothermal pretreatment, the similarity in substrate origin and structural characteristics supports a qualitative comparison with the XOS-extract produced in the present study. Interestingly, butyric acid was observed to be the largest fraction produced by both strains evaluated, with higher values for *L. rhamnosus*. This predominance suggests that, under the conditions evaluated, the metabolism of *L. rhamnosus* favored fermentative pathways directed towards butyrate formation, while *L. acidophilus* showed a lower capacity to produce this compound.

Similar results, in which specific strains of *Lacticaseibacillus rhamnosus* act as strong producers of butyrate in MRS broth, were reported by Thananimit

et al. 2022 who observed concentrations of up to ~37 mM of butyrate for the SD11 strain after 24 h of incubation. It is important to note that, in that study, the cultures were grown in standard MRS medium and no xylooligosaccharides (XOS) were used as the carbon source, nor were the substrates obtained by hydrothermal pretreatment. Therefore, the comparison with the present study, which employs XOS produced by hydrothermal processing, should be regarded as qualitative and restricted to the metabolic potential of the strains rather than to the effect of the substrate itself. Acetic acid showed much lower levels than the other SCFAs, indicating that its formation was limited in the culture medium used or that it was rapidly consumed as an intermediate in other metabolic pathways (Markowiak-Kopec; Ślizewska, 2020). Similarly, propionic acid showed discrete, but slightly higher values in L. rhamnosus, reinforcing that the differences between the strains are also reflected in secondary pathways of carbohydrate metabolism.

The production of SCFAs and medium-chain fatty acids (MCFAs) derived from bacterial metabolism is an important indicator of the fermentative activity and metabolic behavior of probiotic strains (Markowiak-Kopec; Ślizewska, 2020). During growth, species of the genus Lactobacillus can generate different profiles of organic metabolites, especially acetic, propionic, and butyric acids, which play relevant roles in microbial modulation and intestinal health. Furthermore, to classic SCFAs, other medium-chain and branched-chain acids, such as isobutyric, isovaleric, and valeric acids, can be formed, associated with amino acid metabolism and bacterial adaptation to the culture medium. The production of SCFAs, such as acetic, propionic, and butyric acids, is one of the main indicators of colonic fermentation of non-digestible carbohydrates and the metabolic activity of the gut microbiota. These metabolites play an essential role in maintaining the integrity of the intestinal mucosa, modulating pH, and regulating inflammatory and energy processes in the host (Mancabelli *et al.*, 2024 Fusco *et al.*, 2023). MCFAs or branched-chain fatty acids, isobutyric and valeric acids, were the major compounds, especially for *L. rhamnosus*, which showed a more pronounced production profile of these metabolites. The greater formation of branched-chain acids by *L. rhamnosus* suggests a more active metabolism linked to the catabolism of amino acids present in the MRS medium, while *L. acidophilus* exhibited relatively lower values (Liu *et al.*, 2008). However, isovaleric acid showed very low levels in both strains, indicating residual production.

In colonic fermentation assays, the XOS-extract did not increase the PI, which remained negative at all doses tested. However, an increase in Bifidobacterium spp. was observed at low and intermediate doses, furthermore to a reduction in Bacteroides spp., results consistent with studies that report the bifidogenic potential of *Eucalyptus* XOS-extract (Finegold *et al.*, 2014; Lin *et al.*, 2016; Míguez *et al.*, 2021). The absence of an increase in PI may be associated with the presence of residual compounds from HP, such as furfural, hydroxymethylfurfural (HMF), and phenolic derivatives, which can interfere with microbial selectivity, as reported by Broekaert et al. 2011. Therefore, the observed modulation suggests a partial effect that can be amplified in more purified XOS-extracts.

SCFA production in colonic fermentation demonstrated a significant increase in acetic acid and total SCFA at intermediate and high doses, a behavior similar to that reported by Míguez et al. 2011 in the fermentation of XOS-extract from *Eucalyptus nitens*, where acetate was also the main metabolite formed. This increase is indicative of greater saccharolytic activity, consistent with the tendency for a reduction in ammonia levels observed at some doses, suggesting lower proteolytic activity, as reported by Procházková et al. 2023.

Taxonomic characterization indicated a predominance of the phyla Proteobacteria and Actinobacteriota, with a tendency for an increase in Bifidobacteriales and Bifidobacteriaceae after supplementation with XOS-extract, a pattern consistent with the selective stimulus reported by Rivière et al. 2016 and Chung et al. 2016 for non-digestible oligosaccharides. The enrichment of Bifidobacteriales, frequently observed in fermentations with XOS, reinforces the prebiotic potential of the XOS-extract, since bacteria such as Bifidobacterium spp. use XOS as a preferred carbon source, favoring intestinal microbial balance and reducing potentially pathogenic populations (Chung *et al.*, 2016; Rivière *et al.*, 2016). However, microbial alpha diversity remained stable, a common behavior in short-duration fermentations, in which deeper structural changes tend to emerge only after prolonged exposures.

The antioxidant activity of the XOS-extract was intense in the DPPH and FRAP methods, with EC_{50} values lower than those reported for encapsulated or highly purified XOS. Antioxidant action may be associated with both the oligomers themselves, but mainly due to residual phenolic compounds released during HP,

as discussed in studies with *Eucalyptus*-extracts (George *et al.*, 2022; Li, Wei *et al.*, 2020; Vieira *et al.*, 2020). This property adds functional value to the XOS-extract, highlighting a multifunctional ingredient with potential for food applications.

The reduced cytotoxicity (IC_{50}~1497 μg.mL^{-1}) indicates good biocompatibility at moderate concentrations, reinforcing the ingredient's safety for applications in food and supplements. Taken together, the results show that the XOS-extract derived from *Eucalyptus* byproduct has significant functional potential, although its prebiotic effects on the complex microbiota are limited by the extract's purity and the short duration of fermentation. Refinement strategies, standardization, and studies in longer dynamic models can broaden its selectivity and reveal its potential in nutritional and technological applications.

5. CONCLUSION

The results of this study demonstrate that the XOS-extract obtained from *Eucalyptus* byproducts represents a promising and sustainable alternative for the development of dual-action functional ingredients. The XOS-extract showed significant antioxidant activity, low cytotoxicity, and the ability to promote the growth of beneficial bacteria in isolated cultures. Although the modulation of microbiota under short-term colonic conditions was moderate, an increase in Bifidobacterium spp., a reduction in Bacteroides spp., and greater production of SCFAs, indicating a relevant fermentative effect. These findings reinforce that XOS-extract derived from lignocellulosic biomass, even in early stages of purification, have real potential for application in functional foods, prebiotics, and nutraceutical formulations. However, improvements in the purification process and further studies, including dynamic fermentations, long-term evaluations, and more in-depth functional analyses, are essential to maximize its prebiotic selectivity and validate its biological impact. Overall, the XOS-extract studied confirms the biotechnological value of agro-industrial waste and highlights a concrete opportunity to add value to the *Eucalyptus* production chain, contributing to solutions aligned with the circular bioeconomy and innovation in functional ingredients.

Abbreviations

ANOVA	Analysis of variance
AOAC	Association of Official Analytical Chemists
ASVs	Amplicon sequence variants
BCRJ	Banco de Células do Rio de Janeiro
CDS	Chromatography Data System
CFU	Colony-forming units
DMEM	Dulbecco's Modified Eagle's Medium
DMSO	Dimethyl sulfoxide
DP	Degree of polymerization
DPPH	2,2-diphenyl-1-picrylhydrazyl
EtOAc	Ethyl acetate
FASTQ	Raw sequencing files
FID	Flame ionization detector
FOS	Fructooligosaccharides
FRAP	Ferric reducing antioxidant power
GC	Gas chromatography
GOS	Galactooligosaccharides
HH	Hemicellulosic hydrolysate
HMF	Hydroxymethylfurfural
HP	Hydrothermal pretreatment
IC_{50}	Concentration that reduces cell viability or substrate by 50%
ITS	Internal transcribed spacer
LLE	Liquid–liquid extraction
MCFA	Medium-chain fatty acids
MRS	Man, Rogosa and Sharpe (culture medium)
NH_4^+	Ammonium ion
OD_{600}	Optical density at 600 nm

PE250	Paired-end 250 bp sequencing
PI	Prebiotic index
QIIME2	Quantitative Insights Into Microbial Ecology 2
SCFA	Short-chain fatty acids
SEM	Standard error of the mean
TPTZ	2,4,6-tris(2-pyridyl)-s-triazine
UV-Vis	Ultraviolet–visible spectrophotometry
XOS	Xylooligosaccharides

REFERENCES

AACHARY, A. A.; PRAPULLA, S. G. Xylooligosaccharides (XOS) as an emerging prebiotic: microbial synthesis, utilization, structural characterization, bioactive properties, and applications. ***Comprehensive Reviews in Food Science and Food Safety***, v. 10, n. 1, p. 2–16, 2011.

ALVAREZ, V. M. Z.; FERNÁNDEZ, P. V.; CIANCIA, M. Structure–antioxidant activity relationship of xylooligosaccharides obtained from carboxyl-reduced glucuronoarabinoxylans from bamboo shoots. ***Food Chemistry***, v. 455, p. 139761, 2024.

ÁLVAREZ, C. *et al*. In vitro assessment of the prebiotic potential of xylooligosaccharides from barley straw. ***Foods***, v. 12, n. 1, 2023.

ANTOV, M. G.; ĐORĐEVIĆ, T. R. Environmental-friendly technologies for the production of antioxidant xylooligosaccharides from wheat chaff. ***Food Chemistry***, v. 235, p. 175–180, 2017.

ASTM INTERNATIONAL. *Test method for determination of contact pH with activated carbon*. West Conshohocken, PA, 2020.

BIANCHI, F. *et al*. Modulation of gut microbiota from obese individuals by in vitro fermentation of citrus pectin in combination with *Bifidobacterium longum* BB-46. ***Applied Microbiology and Biotechnology***, v. 102, n. 20, p. 8827–8840, 2018.

BROEKAERT, W. F. *et al*. Prebiotic and other health-related effects of cereal-derived arabinoxylans, arabinoxylan-oligosaccharides, and xylooligosaccharides. ***Critical Reviews in Food Science and Nutrition*****,** v. 51, n. 2, p. 178–194, 2011.

BYMYCELL INOVA SIMPLES LTDA. *Relatório de análise de microbiota – Microbiota Illumina*. Ribeirão Preto, 2025.

CARVALHO, A. F. A. et al. Xylo-oligosaccharides from lignocellulosic materials: chemical structure, health benefits and production by chemical and enzymatic hydrolysis. ***Food Research International***, v. 51, p. 75–85, 2013.

CHARTERIS, W. P. et al. Development and application of an in vitro methodology to determine the transit tolerance of potentially probiotic *Lactobacillus* and *Bifidobacterium* species. ***Journal of Applied Microbiology***, v. 84, 1998.

CHUNG, W. S. F. et al. Modulation of the human gut microbiota by dietary fibres occurs at the species level. ***BMC Biology***, v. 14, n. 1, 2016.

CORCORAN, B. M. et al. Survival of probiotic lactobacilli in acidic environments is enhanced in the presence of metabolizable sugars. ***Applied and Environmental Microbiology***, v. 71, n. 6, p. 3060–3067, 2005.

DA SILVA, A. P. et al. Inajá oil processing by-product: a novel source of bioactive

catechins and procyanidins. ***Food Research International***, v. 144, 2021.

DE OLIVEIRA, M. T. *et al*. Restoring balance: probiotic modulation of microbiota, metabolism, and inflammation in SSRI-induced dysbiosis using the SHIME® model. ***Pharmaceuticals***, v. 18, n. 8, 2025.

DIETHER, N. E.; WILLING, B. P. Microbial fermentation of dietary protein. ***Microorganisms***, v. 7, n. 1, p. 19, 2019.

DOSTAL, A. *et al*. Effects of iron supplementation on dominant bacterial groups in the gut. ***British Journal of Nutrition***, v. 112, n. 4, p. 547–556, 2014.

FINEGOLD, S. M. *et al*. Xylooligosaccharide increases bifidobacteria but not lactobacilli. ***Food & Function***, v. 5, n. 3, p. 436–445, 2014.

FUSCO, W. *et al*. Short-chain fatty-acid-producing bacteria: key components of the human gut microbiota. ***Nutrients***, v. 15, n. 9, p. 2211, 2023.

GIBSON, G. R.; ROBERFROID, M. B. Dietary modulation of the human colonic microbiota. ***Journal of Nutrition***, v. 125, n. 6, p. 1401–1412, 1995.

GIBSON, G. R. *et al*. ISAPP consensus statement on the definition and scope of prebiotics. ***Nature Reviews Gastroenterology & Hepatology***, v. 14, p. 491–502, 2017.

HENRIQUES, P. I. A. *et al*. Green process for xylooligosaccharides production using an *Eucalyptus* kraft pulp. ***Journal of Polymers and the Environment***, v. 31, n. 5, p. 2005–2013, 2023.

LIN, S. H. *et al*. Prebiotic effects of xylooligosaccharides on microbiota balance. ***Gastroenterology Research and Practice***, 2016.

MANCABELLI, L. et al. Taxonomic and metabolic development of the human gut microbiome. ***mSystems***, v. 9, n. 4, 2024.

MARKOWIAK, P.; ŚLIŻEWSKA, K. Effects of probiotics, prebiotics, and synbiotics. ***Nutrients***, v. 9, 2017.

MÍGUEZ, B. *et al*. Manufacture and prebiotic potential of xylooligosaccharides from *Eucalyptus nitens*. ***Frontiers in Chemical Engineering***, v. 3, 2021.

MONTANÉ, D. *et al*. Removal of lignin and impurities from xylooligosaccharides. ***Industrial & Engineering Chemistry Research***, v. 45, n. 7, p. 2294–2302, 2006.

MOURE, A. *et al*. Advances in the manufacture and applications of xylooligosaccharides. ***Process Biochemistry***, v. 41, p. 1913–1923, 2006.

OTAVIANO, A. C. A. *et al*. Hydrothermal pretreatment of eucalyptus by-product. ***Separation and Purification Technology***, v. 306, 2023.

PAZ-CEDENO, F. R. ***Hemicellulose biorefinery*. Singapore: Springer Nature**, 2022.

RYCROFT, C. E. *et al*. Fermentation properties of prebiotic oligosaccharides. ***Journal of Applied Microbiology***, v. 91, n. 5, p. 878–887, 2001.

SAMANTA, A. K. *et al*. Xylooligosaccharides as prebiotics from agricultural by-products. ***Bioactive Carbohydrates and Dietary Fibre*,** v. 5, p. 62–71, 2015.

SENDER, R.; FUCHS, S.; MILO, R. Revised estimates for the number of human and bacteria cells. ***PLoS Biology***, v. 14, n. 8, 2016.

SLAVIN, J. Fiber and prebiotics: mechanisms and health benefits. ***Nutrients***, v. 5, p. 1417–1435, 2013.

THURSBY, E.; JUGE, N. Introduction to the human gut microbiota. ***Biochemical Journal*,** v. 474, p. 1823–1836, 2017.

VALLADARES-DIESTRA, K. K. *et al*. The potential of xylooligosaccharides as prebiotics. ***Foods***, v. 12, 2023.

ZHANG, X. *et al*. Coproduction of xylooligosaccharides from sugarcane bagasse. ***Bioresource Technology***, v. 309, 2020

6. SUPPLEMENTARY MATERIAL

Calculation of EC50 and its uncertainty

To calculate EC50 (the value of X when Y=50), we first need to isolate X in the model equation. In the case of the oxidizing agents DPPH and ABTS, the model that best described the reaction kinetics was:

$$Y = a\left(\frac{atan(x - \mu)}{s}\right)$$

This model was chosen because it accurately represents sigmoid kinetics. Model Algebra:

Solving the model equation for x, we obtain:

$$x = \mu + \sigma * tan\left(\frac{y}{a}\right)$$

Therefore:

$$EC50 = \mu + \sigma * tan\left(\frac{y50}{a}\right)$$

Calculation of Uncertainty (Error Propagation): The EC50 is a three-parameter function with uncertainties (a, μ, σ). To find the uncertainty of the EC50 (σEC50), we use the error propagation formula, which is based on the partial derivatives of the function EC50 = f(a, μ, s).

$$\sigma_{\mathrm{EC50}}^2 \approx \left(\frac{\partial f}{\partial a}\right)^2 \sigma_a^2 + \left(\frac{\partial f}{\partial \mu}\right)^2 \sigma_\mu^2 + \left(\frac{\partial f}{\partial s}\right)^2 \sigma_s^2$$

The variance (σEC50) is given by:

(Note: This assumes that the covariances between the parameters are zero, which is the standard approximation when the covariance matrix is not provided).

The derivatives are:

$$\frac{\partial f}{\partial \mu} = 1$$

$$\frac{\partial f}{\partial s} = \tan\left(\frac{50}{a}\right)$$

$$\frac{\partial f}{\partial a} = s \cdot \sec^2\left(\frac{50}{a}\right) \cdot \left(\frac{-50}{a^2}\right) = \frac{-50s}{a^2 \cos^2\left(\frac{50}{a}\right)}$$

The uncertainty value is the standard deviation, defined as the square root of the variance.

Model adopted and quality of fits

For all systems (FRAP and DPPH), the fits showed high values of the coefficient of determination ($R^2 > 0.95$), indicating good adherence of the model to the experimental data. The curves, estimated parameters, EC_{50} values and their respective uncertainties were obtained individually for each sample (XOS, inulin and Trolox).

4 FINAL CONSIDERATIONS

The results obtained in this work confirm that the by-product generated by the pulp industry from *Eucalyptus* can be efficiently converted into XOS with high added value. The application of HP allowed the production of a HH rich in XOS, and the purification strategy using AC stood out as a sustainable, efficient, and viable alternative, promoting high removal of inhibitory compounds without significantly compromising the yield of oligosaccharides.

Furthermore, the XOS-extract is purified using the conventional method (Otaviano *et al*., 2023) showed promising performance in vitro assays, presenting the ability to stimulate beneficial bacteria and antioxidant activity, reinforcing their potential as functional ingredients for food and nutraceutical applications. Therefore this work contributes to the consolidation of the concept of biorefinery applied to forest biomass, by combining technological innovation, environmental sustainability, and the development of products of interest to human health.

REFERÊNCIAS

AACHARY, A. A.; PRAPULLA, S. G. Xylooligosaccharides (XOS) as an Emerging Prebiotic: Microbial Synthesis, Utilization, Structural Characterization, Bioactive Properties, and Applications**. Comprehensive Reviews in Food Science and Food Safety**, v. 10, n. 1, p. 2–16, 2011.

AHMED, W.; LIM, W. **Production of sustainable and structural fiber reinforced recycled aggregate concrete with improved fracture properties.** a review, Elsevier, 2021.

OTAVIANO, C.; *et al*. Hydrothermal pretreatment of Eucalyptus by-product and refining of xylooligosaccharides from hemicellulosic hydrolysate. **Separation and Purification Technology**, v. 306, 2023.

ÁLVAREZ, C.; *et al*. In Vitro Assessment of the Prebiotic Potential of Xylooligosaccharides from Barley Straw. **Foods**, v. 12, n. 1, 2023.

ALVAREZ, V. M. Z.; FERNÁNDEZ, P. V.; CIANCIA, M. Structure-antioxidant activity relationship of xylooligosaccharides obtained from carboxyl-reduced glucuronoarabinoxylans from bamboo shoots. **Food Chemistry**, v. 455, p. 139761, 2024.

BIAN, J.; *et al*. Structural features and antioxidant activity of xylooligosaccharides enzymatically produced from sugarcane bagasse. **Bioresource Technology**, v. 127, p. 236–241, 2013.

BUCKERIDGE, P. **Advances of Basic Science for Second Generation Bioethanol from Sugarcane.** Cham: Springer International Publishing, 2017.

CEBREIROS, F.; GUIGOU, M. D.; CABRERA, M. N. Integrated forest biorefineries: Recovery of acetic acid as a by-product from eucalyptus wood hemicellulosic hydrolysates by solvent extraction. **Industrial Crops and Products**, v. 109, p. 101–108, 2017.

CHEN, T. *et al*. Effects of hydrothermal pretreatment on the structural characteristics of organosolv lignin from Triarrhena lutarioriparia. **Polymers**, v. 10, n. 10, 2018.

CORIM MARIM, A. V.; GABARDO, S. Xylooligosaccharides: prebiotic potential from agro-industrial residue, production strategies and prospects. **Biocatalysis and Agricultural Biotechnology**, v. 37, p. 102190, 2021.

DĄBROWSKI, A.; *et al*. Adsorption of phenolic compounds by activated carbon - A critical review. **Chemosphere**, v. 58, n. 8, p. 1049–1070, 2005.

DE FREITAS, C.; CARMONA, E.; BRIENZO, M. Xylooligosaccharides production process from lignocellulosic biomass and bioactive effects. **Bioactive Carbohydrates and Dietary Fibre**, v. 18, 2019.

DEEHAN, E. C.; *et al*. Revisiting the Concepts of Prebiotic and Prebiotic Effect in Light of Scientific and Regulatory Progress—A Consensus Paper From the Global Prebiotic Association. **Advances in Nutrition**, v. 15, n. 12, p. 100329, 2024.

DEL RÍO, J. C.; *et al*. Differences in the chemical structure of the lignins from sugarcane bagasse and straw. **Biomass and Bioenergy**, v. 81, p. 322–338, 2015.

EK, M.; GELLERSTEDT, G.; HENRIKSSON, G. Pulping Chemistry and Technology. Walter de Gruyter, 2009.

PAZ-CEDENO, F.R. *et al*. **Hemicellulose Biorefinery: A Sustainable Solution for Value Addition to Bio-Based Products and Bioenergy.** Singapore: Springer Nature Singapore, 2022.

GIBSON, G. R. *et al*. Expert consensus document: The International Scientific Association for Probiotics and Prebiotics (ISAPP) consensus statement on the definition and scope of prebiotics, **Nature Publishing Group**, 2017.

KRUSCHITZ, A.; NIDETZKY, B. **Downstream processing technologies in the biocatalytic production of oligosaccharides**, Elsevier Inc., 2020.

LASRADO, L. D.; GUDIPATI, M. Antioxidant property of synbiotic combination of Lactobacillus sp. and wheat bran xylo-oligosaccharides. **Journal of Food Science and Technology**, v. 52, n. 7, p. 4551–4557, 2015.

LEONE, F.; FERRANTE, V. Effects of prebiotics and precision biotics on performance, animal welfare and environmental impact. A review. **Science of The Total Environment**, v. 901, p. 165951, 2023.

LI, B.; YI, Y.; *et al*. Preparation and nutritional properties of xylooligosaccharide from agricultural and forestry byproducts: A comprehensive review.

MANICARDI, T. *et al*. Xylooligosaccharides: A Bibliometric Analysis and Current Advances of This Bioactive Food Chemical as a Potential Product in Biorefineries' Portfolios, **Multidisciplinary Digital Publishing Institute (MDPI)**, 2023.

MHETRAS, N.; MAPRE, V.; GOKHALE, D. Xylooligosaccharides (XOS) as Emerging Prebiotics: Its Production from Lignocellulosic Material. **Advances in Microbiology**, v. 09, n. 01, p. 14–20, 2019.

MOURE, A.; *et al*. **Advances in the manufacture, purification and applications of xylo-oligosaccharides as food additives and nutraceuticals**, 2006.

NERI-NUMA, I. A.; PASTORE, G. M. Novel insights into prebiotic properties on human health: A review. Food Research International, v. 131, p. 108973, 2020.

PINTO, F. *et al*. Model-based optimization of xylooligosaccharides production by hydrothermal pretreatment of Eucalyptus by-product. **Industrial Crops and Products**, v. 154, 2020.

NOGUEIRA-PRIETO, N. M.; *et al*. I. A review of the capacity of xylooligosaccharides to modulate gut microbiota and promote health, **Royal Society of Chemistry**, 2025.

QIN, L. et al. Production of Xylooligosaccharides from Jiuzao by Autohydrolysis Coupled with Enzymatic Hydrolysis Using a Thermostable Xylanase. **Foods**, v. 11, n. 17, 2022.

SAMANTA, A. K.; JAYAPAL, N.; JAYARAM, C.; ROY, S.; KOLTE, A. P.; SENANI, S.; SRIDHAR, M. Xylooligosaccharides as prebiotics from agricultural by-products: Production and applications, **Elsevier**, 2015.

SIVIERI, K. *et al*. Prebiotic Effect of Fructooligosaccharide in the Simulator of the Human Intestinal Microbial Ecosystem (SHIME ® Model). **Journal of Medicinal Food**, v. 17, n. 8, p. 894–901, 2014.

VALLADARES-DIESTRA, K. K. *et al*. The Potential of Xylooligosaccharides as Prebiotics and Their Sustainable Production from Agro-Industrial by-Products, **Multidisciplinary Digital Publishing Institute (MDPI)**, 2023.

VÁZQUEZ, M. J. *et al*. Xylooligo-saccharides: manufacture and applications Production of xylooligosaccharides from ligno-cellulosic materials. ***Trends in Food Science & Technology***, v. 11, p. 387–393, 2000

XAVIER, L. *et al*. Harnessing polyphenols from pulp industry residues of juvenile eucalyptus wood: potential for adhesive applications. **Bioresources and Bioprocessing**, v. 12, n. 1, 2025.

XIAO, L.P.; SONG, G.Y.; SUN, R.C. Effect of Hydrothermal Processing on Hemicellulose Structure. Em: Hydrothermal Processing in Biorefineries. Cham: **Springer** International Publishing, 2017. p. 45–94.

YAO, D.; *et al*. In vitro fermentation of fructooligosaccharide and galactooligosaccharide and their effects on gut microbiota and SCFAs in infants. **Journal of Functional Foods**, v. 99, 2022.

YU, X.; *et al*. Prebiotic Potential of Xylooligosaccharides Derived from Corn Cobs and Their In Vitro Antioxidant Activity When Combined with Lactobacillus**. Journal of Microbiology and Biotechnology**, v. 25, n. 7, p. 1084–1092, 2015.